

<https://doi.org/10.1016/j.cep.2019.03.0171>

NOTICE: this is the author's version of a work that was accepted for publication in Chemical Engineering and Processing: Process Intensification. Changes resulting from the publishing process, such as peer review, editing, corrections, structural formatting, and other quality control mechanisms may not be reflected in this document. Changes may have been made to this work since it was submitted for publication. A definitive version was subsequently published in ENGINEERING AND PROCESSING: PROCESS INTENSIFICATION, [(2019)]doi:10.1016/j.cep.2019.03.0171

Sonocrystallisation: observations, theories and guidelines

Jeroen Jordens^{a,b*}, Bjorn Gielen^{a,b}, Christos Xiouras^a, Mohammed Noorul Hussain^a, Georgios D. Stefanidis^a, Leen C.J. Thomassen^b, Leen Braeken^b, Tom Van Gerven^a

^a Department of Chemical Engineering, KU Leuven, Celestijnenlaan 200F, B-3001 Leuven, Belgium

^b Research group Lab4U, Faculty of Industrial Engineering, KU Leuven, Universitaire Campus gebouw B bus 8, 3590 Diepenbeek, Belgium

*Corresponding author. Address: Celestijnenlaan 200F, 3001 Leuven, Belgium; E-mail address: tom.vangerven@kuleuven.be; tel.: +32 16 32 23 42

Abstract

Crystallization is an important and widely used separation technique in the chemical and pharmaceutical industry. Control of the final particle properties is of great importance for these industries. The application of ultrasound in these crystallization processes, also referred to as sonocrystallization, has shown to impact nucleation, crystal growth and fragmentation. As a result this technology has potential to control the final particle size, shape and polymorphic form.

This review provides a comprehensive overview of the recent advances in sonocrystallization. It reviews the observed effects of ultrasound on the different stages of the crystallization process. Recent insights in the mechanism behind these effects are discussed as well. Finally, guidelines for the operating conditions, such as ultrasonic frequency, power, type of cavitation bubbles, time window and moment of application are formulated.

Keywords

Sonocrystallization, ultrasound crystallization, sononucleation, sonofragmentation, ultrasound-assisted nucleation, ultrasound-assisted growth

1. Introduction

Crystallization is a widely used technique for the production and separation of pharmaceuticals and fine chemicals [1–3]. During crystallization, multiple mechanisms are, often simultaneously, active such as primary and secondary nucleation (attrition), crystal growth and agglomeration [4]. Design and control of these crystallization processes is complicated because of the strict requirements related to the final product attributes [5]. The application of ultrasound to crystallization processes can help to gain control over nucleation, crystal growth and fragmentation and therefore impact the particle size distribution, crystal shape and polymorphic form [3,6–10]. Ultrasound can be defined as mechanical sound waves with frequencies of 20 kHz up to several GHz [11]. This frequency region can further be divided into two sub-regions, namely power ultrasound and diagnostics. The former uses lower frequencies between 20 kHz and 5 MHz, where a larger amount of acoustic energy can be generated to induce cavitation bubbles in the liquid. The effects originating from these cavitation bubbles are mostly used to intensify chemical processes. Diagnostic ultrasound comprises frequencies of 5 MHz or above since these frequencies do not produce cavitation and are therefore perfectly suited for medical imaging [11]. Ultrasound irradiation of a solution results in pressure waves in the liquid which cause compression and rarefaction of liquid molecules. Above a critical acoustic pressure of about 10^{10} Pa, voids called cavitation bubbles will be created in water [12,13]. In practice, however, impurities or microbubbles of dissolved gasses will be present in the liquid. These bubbles act as nuclei and lower the required pressure for the creation of cavitation bubbles [14]. Furthermore, at high frequencies, acoustic streaming can occur. At these high frequencies, vibrating liquid molecules have less time to revert to their equilibrium positions before the next disturbance. When the next ultrasonic pulse encounters the liquid molecules before they are

fully relaxed, the molecules will move in the direction of the wave propagation and cause acoustic streaming.

The first article on the application of ultrasound waves to crystallization processes was published in 1927 by Richards and Loomis [15]. Over decades, literature showed that the creation of cavitation bubbles by applying power ultrasound during crystallization processes (sonocrystallization) enables positive effects like smaller metastable zone widths (MZW), shorter induction times, the formation of smoother and smaller particles and increased reproducibility of the particle size distributions [6,16–20]. Also, more and more efforts were performed to gain insight into the mechanisms behind sonocrystallization. Hem reviewed possible mechanisms of ultrasound-assisted crystallization in 1967 based on these earliest publications [20]. This review stimulated more work directed into gaining additional insights into the mechanisms behind sonocrystallization. Although recent review papers on sonocrystallization exist, most of these reviews focus on the observed effects of ultrasound on nucleation and fragmentation and touch only briefly the studied mechanisms behind sonocrystallization [19,21–25].

The aim of this review is to provide a comprehensive overview of the state-of-the-art literature and scientific knowledge in the field of sonocrystallization. It provides an extensive overview of the observed effects of ultrasound on primary, and secondary nucleation as well as crystal growth, sonofragmentation, the polymorphic form and crystal shape. In addition, it discusses the recent insights obtained on the mechanisms behind these observed effects. Finally, guidelines for operating parameters such as the ultrasonic frequency, power, type of cavitation bubbles, the time window in which ultrasound is best applied and the moment of application are also discussed.

2. Observations and theories on ultrasound-assisted crystallization

2.1.Nucleation

The effects of ultrasound on crystallization process are primarily visible on the nucleation step of the crystallization process. Nucleation is considered as the birth of crystals in a solution and is responsible for the initial crystal population that will later go through growth, agglomeration and breakage processes, to form the final crystalline product [4]. Nucleation can be classified in primary and secondary nucleation [4,26]. The former is defined as the formation of new crystals from solution. When there is already crystalline matter of the solute present, it is classified as secondary nucleation. Primary nucleation can be further divided in primary homogeneous and heterogeneous nucleation. Primary nucleation is homogeneous when it occurs in a clear particle-free solution. When foreign particles or surfaces of the equipment initiate nucleation, it is classified as primary heterogeneous nucleation. Several papers in literature report on the effects of ultrasound on these different classes of nucleation [3,6,27–39]. First the observed effects will be discussed and next the possible mechanisms.

2.1.1. Observed effects of ultrasound on nucleation

I Primary homogeneous nucleation

Primary homogeneous nucleation, *e.g.* spontaneous nucleation without the presence of solid particles or crystals, is clearly affected by ultrasound. Multiple articles report a decrease in the induction time, nucleation at lower supersaturation or a reduction in the Metastable Zone Width (MZW) upon sonication [3,33,36,37,39–43]. Moreover, ultrasound increases the reproducibility of the induction time, cloud points and MZW measurements [22,24,39,44]. The

magnitude of this reduction in MZW, compared to non-sonicated conditions, depends on the applied cooling rate. Bari *et al.* showed that during the cooling crystallization of K_2SO_4 , the reduction in MZW by application of ultrasound is larger for low cooling rates compared to high cooling rates [40]. A 20 kHz probe delivering 51 W of calorimetric power to a 250 mL vessel was used in these experiments. The initial saturation temperature corresponded to 60 °C. At a cooling rate of 0.5 °C/min, the MZW decreased by 1.7 °C from 12.6 °C for conventional crystallization to 10.9 °C for sonocrystallization. This reduction in MZW decreased to 0.6 °C for a cooling rate of 2 °C/min and became negligible (-0.1 °C) for a cooling rate of 3 °C/min. Ultrasound has thus a larger effect on the MZW at lower cooling rates. A similar observation was made by Hazi Mastan *et al.* during the cooling crystallization of *L*-phenylalanine [43]. Also here a 20 kHz probe was used but now in a 500 mL vessel and with 180 W of electrical power. Moreover, in this paper five different saturation temperatures were tested from 20 °C to 60 °C with a step size of 10 °C. For all saturation temperatures, the reduction in MZW was the largest at the lower cooling rates.

Additionally, the supersaturation ratio at which ultrasound is applied plays an important role. Induction time experiments with sodium sulfate and roxithromycin showed that the reduction in induction time by application of ultrasound is larger at low supersaturation ratios compared to higher supersaturation ratios [29,45]. Figure 1 shows the evolution of the induction time as function of the supersaturation ratio as observed by Guo *et al.* during the ultrasound-assisted antisolvent crystallization of roxithromycin [45]. The induction time under silent conditions is much higher for low supersaturation ratios compared to high supersaturation ratios. Consequently, the room for improvement or reducing this induction time is larger at the lower supersaturation ratios. At a supersaturation ratio of five, the observed reduction in the induction time is about 500 s while at a supersaturation ratio of 2.5 the reduction is more than 4000 s.

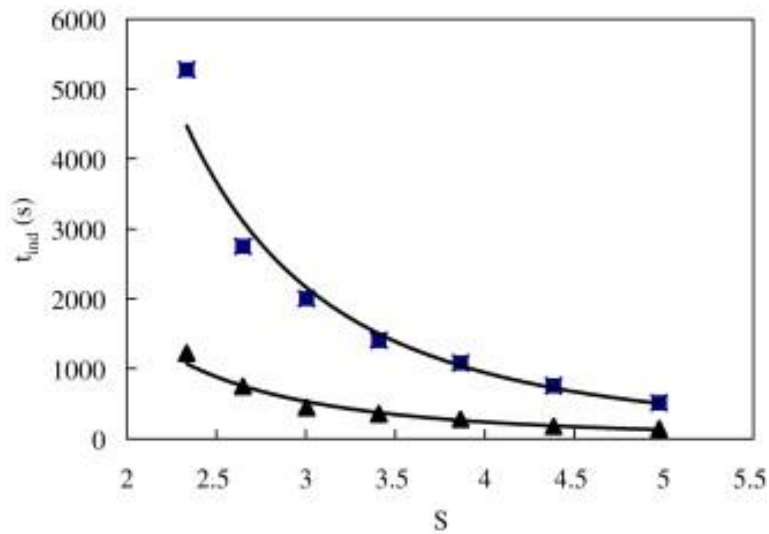


Figure 1 . Influence of ultrasound on the induction time of roxithromycin: (▲) with ultrasound, (■) without ultrasound. Reprinted from Journal of Crystal Growth, 273, Z. Guo,M. Zhang,H. Li,J. Wang,E. Kougoulos, Effect of ultrasound on anti-solvent crystallization process, 555-563., Copyright (2018), with permission from Elsevier [45].

Furthermore, Bari *et al.* and Hazi Mastan *et al.* performed kinetic studies on the impact of ultrasound on the nucleation rate and apparent order of nucleation. Bari *et al.* used a gPROMS parameters estimation in two steps while Hazi Mastan *et al.* compared four different approaches namely the Nyvlt's approach, Sangwal's self-consistent Nyvlt-like equation, Sangwal's classical three dimensional nucleation theory approach and Kuboto's model. The Nyvlt's approach is the classical one which estimates nucleation kinetics based on the MZW. However, the nucleation order and nucleation rate constant of the Nyvlt's equation have no physical significance [43]. Furthermore, Sangwal argued that a number-based nucleation rate would be more convenient than the mass-based nucleation rate in the Nyvlt approach [43]. Sangwal proposed therefore two different approaches, a self-consistent Nyvlt-like equation and a three

dimensional nucleation theory approach. The former relates the nucleation rate with the maximum supersaturation via a power law expression instead of the complicated unit of Nyvlt's nucleation constant. The latter is derived from the classical 3D nucleation theory but expresses the nucleation rate on a number basis. All previous techniques use MZW data. The measurement of the MZW depends, however, on the detection technique in a given system. Kubota proposed therefore a new model where the MZW is described as the supercooling at which the number density of grown nuclei reaches a fixed but unknown value. All approaches led to the same conclusion that ultrasound decreases the apparent nucleation order and increases the nucleation rate significantly. An increase in nucleation rate by one order of magnitude was reported by both authors [40,43].

A reduction of the particle size and narrowing of the crystal size distribution (CSD) are also commonly reported effects of the application of ultrasound during crystallization processes [29,40,42]. These effects are often related to the increase in nucleation rate. Higher nucleation rates lead to the production of more nuclei which grow into more but smaller crystals in the end.

II Primary heterogeneous nucleation

It is practically impossible to remove completely all solid matter from a solvent or a solution. As a consequence, heterogeneous nucleation will always occur to some extent [4,32]. There exists a critical supersaturation level above which the rate of homogeneous nucleation is larger than the rate of heterogeneous nucleation. Guo *et al.* identified this critical supersaturation level for the reactive crystallization of BaCl₂ and Na₂SO₄ and tested the effect of ultrasound on both the primary homogeneous and heterogeneous nucleation [32,33]. A titanium probe, with an unspecified frequency, was operated at electrical power levels of 8.6 to 46.0 W. They observed

a reduction in induction time for both types of nucleation. Figure 2 shows plots of $\ln^{-2}(S)$ vs $\ln(t_{in})$ with S , the super saturation ratio (-) and t_{in} the induction time (s). Zone I is characterized by the dominance of homogeneous nucleation while in zone II heterogeneous nucleation is the main nucleation mechanism. These two zones can be distinguished from each other by the slope of t_{in} as function of $1/\ln^2 S$ as can be seen in Figure 2. The slope at higher supersaturation levels, so low values of $1/\ln^2 S$ and homogeneous nucleation, is significantly higher than the slope at lower supersaturation levels where heterogeneous nucleation is thought to be the main nucleation mechanism. A significant reduction in induction time with an increase in ultrasound power was observed for both homogeneous and heterogeneous nucleation. Similar observations were also made by Zeng *et al.* during the cooling crystallization of sodium sulfate [29]. Here, an ultrasound probe system was used at a fixed frequency of 20 kHz. The electrical power input was varied from 0 to 130 W. These results indicate that ultrasound increases the nucleation rates of both homogeneous and heterogeneous nucleation. Furthermore, one can observe that the difference in $\ln(t_{in})$ is the largest at higher $\ln^{-2}(S)$ values and thus lower supersaturation ratios. This again shows that the reduction in induction time is the largest at the lowest supersaturation ratios as discussed in the previous section.

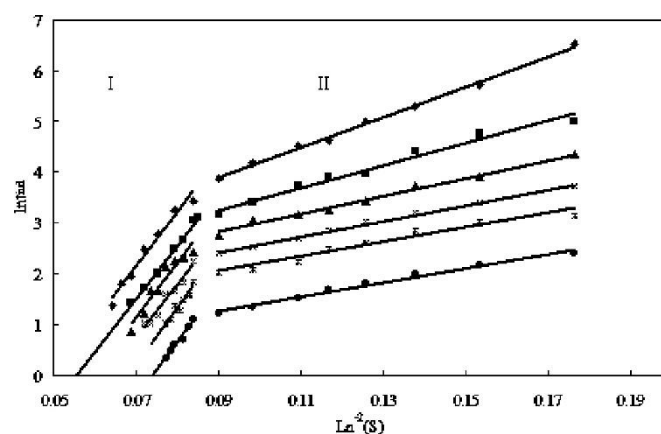


Figure 2. The plots of $\ln^{-2}(S)$ vs $\ln(t_{ind})$. At zone I, when nucleation is predominantly homogeneous: (◆) the experimental data without ultrasound, (■) the experimental data with

the energy input of 8.622W, (▲) the experimental data with the energy input of 17.962W, (×) the experimental data with the energy input of 27.302W, (*) the experimental data with the energy input of 36.642W, and (●) the experimental data with the energy input of 45.982W. At zone II, when nucleation is predominantly heterogeneous: (◆) the experimental data without ultrasound, (▲) the experimental data with the energy input of 8.622W, (▲) the experimental data with the energy input of 17.962W, (×) the experimental data with the energy input of 27.302W, (*) the experimental data with the energy input of 36.642W, and (●) the experimental data with the energy input of 45.982W. Reprinted from: Z. Guo; A. G. Jones; H. Hao; B. Patel; N. Li; Journal of Applied Physics 2007, 101, DOI: 10.1063/1.2472652, with the permission of AIP Publishing [32].

Kim *et al.* studied the nucleation kinetics during the cooling crystallization of 3-Nitro-1,2,4-triazol-5-one [30]. They found that primary heterogeneous nucleation was the dominating mechanism during their crystallization process. Similar to primary homogeneous nucleation, ultrasound increases the nucleation rate by a factor of more than 10 compared to the same crystallization with a mechanical stirrer. These results indicate that ultrasound is able to increase the nucleation rate one order of magnitude for both primary homogeneous and heterogeneous nucleation.

III Secondary nucleation

The majority of the papers about ultrasound assisted crystallization focusses solely on the effects of ultrasound on primary nucleation. The effects of ultrasound on secondary nucleation are much less studied. Secondary nucleation involves the production of new crystals in a

solution containing pre-existing crystalline matter from the solute. Secondary nucleation can occur either by the crystals acting as templates for new crystal nuclei to be formed or by the crystals fragmenting to produce more nucleation sites [23,24]. Despite the lack of numerous studies, the few papers which did study secondary nucleation upon sonication show clear effects [24,40,41]. Bari *et al.* simulated the sono-crystallization kinetics during the cooling crystallization of K_2SO_4 in water [40]. The simulations indicate that breakage plays an important role during sonocrystallization in addition to the increase in nucleation rates as discussed before. A similar observation was also made by Chow *et al.* during an experimental study of ice crystallization in sucrose solutions [46]. Microscope images showed that dendrites, located at the end of the crystals, were broken into fragments by the cavitation bubbles burst. These fragments acted as new crystal nucleation sites and hence induced secondary nucleation. This breakage of existing crystals and subsequent induction of secondary nucleation is also expected for organic and inorganic crystals during crystallization from a supersaturated solution [40,41,47,48].

As a conclusion, ultrasound is able to reduce the MZW and induction time significantly, especially at low supersaturation ratios. The lower the supersaturation ratio, the larger the effect of ultrasound on induction time. This effect was visible for both primary homogeneous and heterogeneous nucleation. These reductions in MZW and induction times were visible for cooling crystallization, as well as anti-solvent and evaporative crystallization. The observed effects of ultrasound on nucleation can therefore be considered independent of the type of crystallization.

2.1.2. Mechanisms behind ultrasound assisted nucleation

Despite the numerous observations, explained in the previous section, the mechanism behind ultrasound enhanced nucleation is still unknown. Several mechanisms are proposed in literature and all agree that the effect is not caused by the sound waves directly but by acoustic streaming or by the cavitation bubbles generated by the ultrasound field [20,49–51]. Acoustic streaming can be considered as a fluid flow generated by attenuation of an acoustic wave [52,53]. In an ideal fluid, the time-averaged particle displacement (net fluid flow), when subjected to an acoustic field, is zero everywhere. In a real fluid, in contrast, viscous attenuation occurs which causes the net displacement of fluid particles during each cycle of an oscillation. As a result, the net displacement becomes non-zero and a global formation of streaming flows can be developed. Three different types or subcategories of acoustic streaming can be defined, namely boundary layer acoustic streaming (Schlichting and Rayleigh streaming), Eckart streaming in the bulk fluid and cavitation microstreaming [52,53].

Boundary layer acoustic streaming is created when an acoustic wave is created parallel to a solid interface. Because of the no-slip condition at the walls and the corresponding steep velocity profile, significant differences in viscous dissipation between the walls and the bulk occur. This results in spatially fixed pressure nodes and antinodes, which leads to a steady vortical fluid motion in the boundary layer (Schlichting streaming) [53]. These vortices in the inner boundary layer create counter-rotating vortices in the outer boundary layer (Rayleigh streaming).

Eckart streaming is created by dissipation of acoustic energy in the bulk of the liquid. This results in a steady momentum flux which creates a jet of fluid inside the acoustic beam in the direction of the acoustic wave propagation [52].

Cavitation microstreaming is considered the flow formed by acoustically driven oscillations of microbubbles in a liquid [53]. These oscillations are transferred via the boundary layer surrounding the bubble and generate vortices and convective motion in the fluid. In addition also stress fields, which largely depend on their mode of oscillation, are created in the surrounding of the oscillating bubbles.

A fourth form of streaming which can be induced by ultrasound waves is surface acoustic wave induced streaming [52]. This type is induced by interdigital transducers which create a pressure wave in a fluid compartment (droplet). Acoustic streaming is created in the droplet by viscous attenuation.

Cavitation bubbles are created by an ultrasound field when the negative acoustic pressure exceeds the local tensile strength of the liquid and hence the molecules are pulled apart from each other. In reality, impurities such as dissolved gas bubbles or microbubbles will be present in the liquid which lower the threshold for creation of cavitation bubbles. Cavitation bubbles are mainly classified in two types, namely stable and transient bubbles [12,54]. In this paper we follow the classification as proposed by Ashokkumar [55]. Stable cavitation refers to bubbles which show a high energy collapse where the same bubbles repetitively collapse and grow several times [55]. Transient bubbles show also a high energy collapse but are followed by fragmentation and the creation of new cavitation nuclei. Ashokkumar showed via multi bubble sonoluminescence that transient bubbles existed only for one or a few acoustic cycles whereas stable bubbles existed for hundreds of acoustic cycles [56]. The high energy collapse of both transient and stable bubbles can result in the simultaneous generation of local hot spots and high pressures, shockwaves, acoustic streaming, liquid jets, sonoluminescence and the production of radicals [12,35,57]. All these effects occur simultaneously, which makes it difficult to identify a single effect as the cause for the increase in nucleation rate. Several papers

investigated the mechanism behind sonocrystallization. The different hypotheses proposed in literature will be discussed below.

I Primary homogeneous nucleation

The most commonly proposed mechanisms to explain the spontaneous primary homogeneous nucleation are the hypotheses of cooling, pressure, evaporation, segregation, and flow induced nucleation [9,20,51,58].

1. Cooling hypothesis

The cooling hypothesis states that during the expansion phase of the cavitation bubble, evaporation occurs from the surface of the cavitation bubble to the bubble interior. As a result, the surface is cooled and it is suggested that this cooling causes local supersaturation and hence nucleation. This theory, also referred to as the Hickling theory, is the most commonly cited theory in the field of ultrasound for food applications [22]. Calculations of the temperature drop by evaporation showed, however, that it was limited to 1°C for bubbles of 100 µm, a typical size for cavitation bubbles generated at around 30 kHz [20,59]. This cooling of 1°C is too small to cause nucleation [20]. For higher frequencies, the bubble size is even smaller which consequently results in less expansion and hence a smaller cooling effect. However, significant reductions in MZW were observed in literature at frequencies above 30 kHz [50,60]. Therefore, it is believed that this cooling effect is too small to have a significant effect on nucleation. In addition, nucleation is expected to occur immediately after collapse according to this theory. High speed photography experiments show, however, that there is a delay between the cavitation and the occurrence of ice nucleation [61,62]. A delay of 0.5 s between the onset of sonication and the detection of nucleation was observed.

2. Pressure hypothesis

Upon bubble collapse, high pressures up to 1 GPa are created in the surrounding liquid [20]. As most components show a decreased solubility at elevated pressures, these high pressures are thought to result in an increased supersaturation and hence enhanced nucleation [20]. The increase in supersaturation, defined as the difference between the liquid temperature and melting temperature (solid-liquid transition), was simulated by Cogné *et al.* for different initial bubble radii and acoustic pressures for the nucleation of ice [63,64]. Significant local supersaturations of -370 K were obtained at the time of maximum pressure at the bubble wall. This increase of the supersaturation was caused by the change in melting temperature at higher pressures. The huge supersaturations are thought to trigger nucleation even though the high supersaturation domain (>-50 K) is very narrow in time (around 1 ns after the collapse) and space (around 2 μm from the bubble wall). Simulations in the same papers suggested namely that nucleation could be triggered starting from a supersaturated solution of 5 K for bubbles with initial radius of 5 μm driven by an ultrasonic sinusoidal wave with a frequency of 29 kHz and acoustic pressure amplitude of 220 kPa [64]. Brotchie *et al.* reported, however, conflicting results with this pressure hypothesis [59]. Experiments with zinc sulphate heptahydrate, for which solubility is independent of the pressure, show significant lower induction times during sonication compared to silent conditions [51]. This indicates that more research is needed to validate for which components this theory holds true.

3. Evaporation hypothesis

During growth of the cavitation bubble, solvent can evaporate to the interior of the cavitation bubble, as already discussed under the cooling hypothesis. This may not only induce cooling at the bubble surface but may also produce a depletion layer of solvent near the bubble wall. As a result, the solute concentration, and hence supersaturation, is thought to increase locally at this

bubble wall [51]. The evaporation hypothesis assumes that this depletion layer, rather than the cooling effect, triggers nucleation. Wohlgemuth *et al.* tested this hypothesis during crystallization experiments with dodecanedioic acid in propyl acetate, ethyl acetate and acetonitrile [65]. Gas bubbles were introduced in the setup which causes a significant reduction of the MZW. Next, these gas bubbles were saturated with the different solvents to avoid evaporation of solvent into the bubble. These experiments yielded similar MZWs as during the unsaturated experiments. Therefore, it was concluded that heterogeneous nucleation, with the cavitation bubbles as nucleation center, rather than solvent evaporation, was the main mechanism behind these observations. This theory will be further discussed in the section on primary heterogeneous nucleation.

4. Segregation hypothesis

When a cavitation bubble collapses, the inward motion of the liquid is stopped violently by the gas recompression in the bubble. As a result, a huge outward acceleration of the liquid is created. Molecules with different densities will not be accelerated to the same extent. Compound clusters, denser than the surrounding solvent molecules, will accelerate slower and are hence segregated from the solvent molecules. As a result, these clusters become supersaturated near the bubble wall for a very short time (ca. 1 ns) and therefore their direct collisions are promoted and nucleation is enhanced [51]. This hypothesis assumes that the compound is denser than the solvent. The larger the density difference between these compounds and the solvent, the faster nucleation should occur. In order to get an idea of the segregation phenomenon, the segregation parameter $\tilde{\beta}$ can be calculated using Eq. 1 [66].

$$\text{Eq. 1} \quad \tilde{\beta} = \frac{N_{av}\rho_A V_A}{RT} \left(\frac{1}{\rho_A} - \frac{1}{\rho_{solvent}} \right)$$

Herein, N_{av} denotes Avogadro's number ($6.022 \cdot 10^{23}$ 1/mol), ρ_A the particle density (kg/m^3), V_A the volume of particle A (m^3), R the universal gas constant ($8.314 \text{ J}/(\text{mol K})$), T the temperature (K) and $\rho_{solvent}$ the density of the solvent (kg/m^3).

When $\tilde{\beta}$ becomes 0, the mixture will be unsegregated (i.e. perfectly uniform). When $\tilde{\beta} < 0$ (A is the heaviest species), component A will be **concentrated** at the bubble wall and the mixture will be overconcentrated at each bubble collapse. When $\tilde{\beta} > 0$ (A is lightest species), no improvement of the nucleation rate should occur as the solvent gets overconcentrated at the bubble wall.

This hypothesis was tested via numerical simulations and some exploratory tests. The numerical simulations showed results in accordance with this segregation theory [67]. Our research group performed, however, cooling sonocrystallization experiments with paracetamol and 3,5 dimethylpyrazole (DMP) at 41 kHz and 53 W/L [27]. Paracetamol has a density higher ($1,26 \text{ kg/m}^3$; $\tilde{\beta} = -2.69 \cdot 10^{-4}$) than the solvent (water), while DMP has a density lower ($0,88 \text{ kg/m}^3$; $\tilde{\beta} = 1.24 \cdot 10^{-4}$) than the solvent. According to the segregation theory, one would expect that ultrasound reduces the MZW for paracetamol and has no effect for DMP. Jordens observed, however, that ultrasound reduced the MZW significantly for both paracetamol and DMP [27]. This indicates that other theories besides the segregation theory should be valid as well. An extensive experimental study is, however, required to validate or invalidate this segregation theory.

5. Convection induced nucleation

Ultrasound waves can create turbulences in the fluid via shockwaves or acoustic streaming as described before. In this hypothesis of flow induced nucleation, it is believed that these turbulences enhance the nucleation rate. It is, however, unclear how this flow streams create

this effect. Some authors claim that the flow streams trigger collisions of molecules and hence increase the creation of clusters of molecules [9,61]. As a result, more nuclei are formed and the nucleation rate is increased. Nalajala *et al.*, for example, reported that intense convection in an aqueous solution of KCl increased the nucleation rate [9]. In their experiments, both mechanical and ultrasound induced flow streams enhanced nucleation rates. The convection in a sonicated system has two components, namely shockwaves and microturbulence. The former are created upon bubble collapse when the inward bubble motion comes to a sudden halt when the minimum radius is reached. At that moment, liquid molecules converging to the bubble center are reflected back and induce shockwaves. Microturbulence is created by the oscillatory movement of the cavitation bubbles in the ultrasound field. These vibrations generate turbulences in the liquid around the bubble, known as microturbulences. Nalajala and Moholkar found during their experiments that shockwaves enhance the nucleation rate while microturbulences improve the growth rate [9]. The pressure shockwaves accelerate solute molecules with high force so that these molecules collide with each other and clusters of molecules are created which overcome the surface and volume free energy barrier for nucleation [40]. The enhancement of nucleation rate by the shockwaves was, however, more pronounced than the improvement of crystal growth by microturbulence.

Others state that the turbulences generated via acoustic streaming increase the heat and mass transfer or diffusion coefficient D_{AB} [24,33,40,62,68–70]. In evaporative crystallization, the increased heat and mass transfer lead to faster evaporation of the solvent and hence supersaturation is created faster which results in higher nucleation rates [68]. During anti-solvent crystallization this leads to a uniform and rapid mixing of the solvent and anti-solvent [69,70]. As a result, the solubility is decreased and nucleation of crystals is triggered. Zhang *et al.* suggested convection or flow induced nucleation as the driving mechanism for the nucleation of ice in water [62]. The particle image velocimetry (PIV) experiments performed

in that paper showed that the time between the onset of sonication and nucleation was similar to the time required for the flow to develop.

As a conclusion, some doubts can be placed on the hypotheses of cooling, pressure, evaporation and segregation. The theory of convection induced nucleation is also not incontestably proven in literature but, unlike the previous theories, there are, to the authors' best knowledge, no articles reporting conflicting results with this theory. It is, however, very likely that ultrasound shifts nucleation from the homogeneous subclass to the heterogeneous class or even secondary nucleation as will be discussed in the following sections.

II Primary heterogeneous nucleation

It is already well known that the presence of foreign particles, such as dust particles, in a liquid lowers the required work to form clusters of a critical size and hence enhances the nucleation rate [36,71,72]. In the hypothesis of the bubble as nucleation center, it is assumed that cavitation bubbles act similarly as these foreign particles and hence introduce heterogeneous nucleation. Wohlgemuth *et al.* tested this hypothesis by introducing synthetic air gas bubbles in a supersaturated solution [50,65]. Gassing of solutions of dodecanedioic or adipic acid in propyl acetate, ethyl acetate and acetonitrile resulted in significant reductions of the MZWs in all experiments. This effect could be explained by either heterogeneous nucleation or evaporation of solvent in the gas bubble. The latter was excluded by experiments with saturated gas bubbles as explained before.

Furthermore, a model was proposed in literature which simulates the heterogeneous nucleation by ultrasound based on the contact angle [36]. The free energy required for heterogeneous

nucleation (ΔG_{het}) relates to the free energy needed for homogeneous nucleation (ΔG_{hom}) by the following equation [32].

$$\text{Eq. 2} \quad \Delta G_{het} = f \Delta G_{hom}$$

The geometric correction factor $f(-)$ is a function of the contact angle θ ($^\circ$) which is the angle between the crystalline deposit and the foreign solid surface [32].

$$\text{Eq. 3} \quad f = \frac{(2 + \cos \theta)(1 - \cos \theta)^2}{4}$$

Figure 3 shows a graphical representation of the contact angle between the crystal and foreign solid surface.

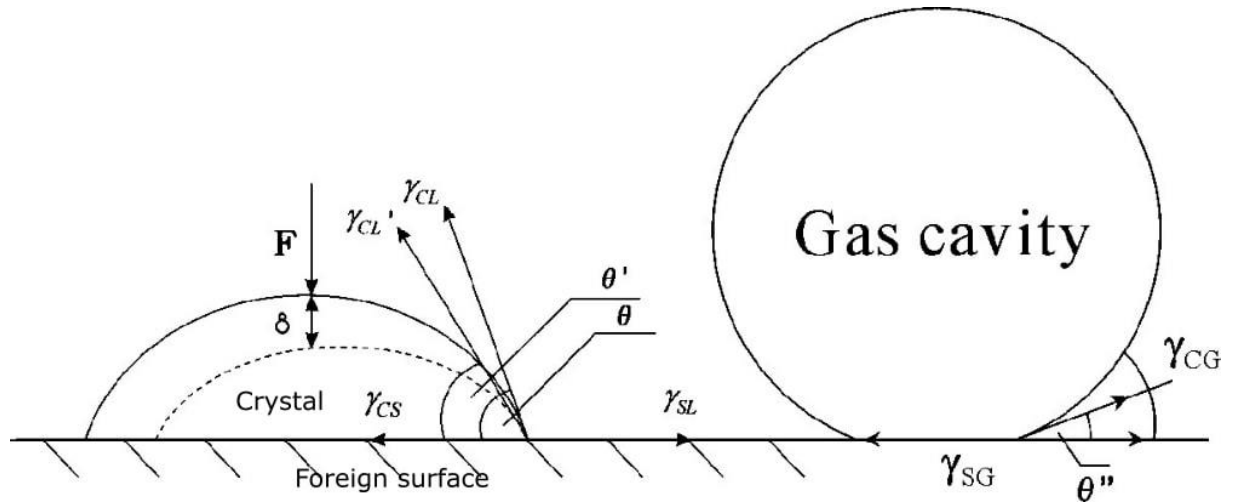


Figure 3. The influence of ultrasound on contact angle (θ). The force compressing the crystal F and the nucleation process occurring at bubble/solution/foreign solid interface are predominant reasons why contact angle (θ) decreases with the increase of energy input. Reprinted from: Z. Guo; A. G. Jones; H. Hao; B. Patel; N. Li; Journal of Applied Physics 2007, 101, DOI: 10.1063/1.2472652, with the permission of AIP Publishing [32].

According to Guo *et al.* and Wohlgemuth *et al.*, ultrasound is able to impact this contact angle and therefore the geometric correction factor f and hence the energy barrier for nucleation [32,65]. Furthermore, Guo *et al.* investigated the effect of the energy input on this contact angle and geometric correction factor f [32]. Figure 4 shows the plots for f and θ in function of the energy input. It was found that both f and θ decrease with the energy input. However, also the gradient of f and θ decreases with the increase in energy input. A given increase in ultrasonic energy has thus a smaller effect on f and θ at high energy inputs compared to low energy inputs. Guo *et al.* formulated three possible explanations for the change in contact angle with the energy input [32].

First, imploding cavitation bubbles create shockwaves which may induce forces on the nuclei. This force (F) is visualized in Figure 3 and can compress the crystal and change the crystal shape. This will reduce the value of the contact angle from θ into θ' . This can be explained by the interfacial tensions between the solid and the liquid (γ_{CL}), between the solid crystalline phase and the foreign solid surface (γ_{CS}) and between another foreign solid surface and the liquid (γ_{SL}). Resolving these forces in the horizontal direction yields the following equation:

$$\text{Eq. 4 } \gamma_{SL} = \gamma_{CS} + \gamma_{CL} \cos \theta$$

The force working on the crystal, changing the crystal shape, will be balanced by a change in interfacial tension to reach a new equilibrium. The higher the energy input, the larger the shockwaves become, the larger the forces on the nuclei and hence the smaller the contact angle becomes [12,32].

The decrease of the contact angle and geometric correction factor f can also be related to the cavitation bubbles themselves. Heterogeneous nucleation can namely occur on a foreign solid surface, at the cavitation bubble/solution interface and at the bubble/solution/foreign solid

surface interface. An increase in energy input will result in more cavitation bubbles and hence more useful sites for crystal nucleation. Additionally, an increase in energy can also increase the vibration intensity of cavitation bubbles. The higher the vibration intensity, the more resistance, composed of interfacial tension and the force between solvent molecules, should be overcome. This second possible explanation assumes that nucleation occurs at the bubble/solution interface. The higher the energy input, the higher the interfacial tension between the liquid and the cavitation bubble and between the solid crystalline phase and cavitation bubbles becomes. Consequently, the contact angle θ is changed as well.

The third option assumes that nucleation occurs at the bubble/solution/foreign solid surface interface which is also shown in Figure 3. The rise in energy input will affect in this case both the bubble diameters and the interfacial tensions. Both can influence the contact angle θ [12,32]. Guo *et al.* pointed out that, for heterogeneous nucleation, the nucleation rate at the cavitation bubble/solution interface is normally lower than the homogeneous nucleation rate. Therefore, it was concluded that the second reason should not be the main reason. Moreover, simulations indicated that the force from the bubble implosions cannot be the only reason to explain the change in contact angle and geometric correction factor with energy input. It is therefore believed that also nucleation occurring at the bubble/solution/foreign solid surface contributes to the drop in contact angle.

An alternative explanation for primary heterogeneous nucleation could be the alignment of crystal faces at the solvent - bubble interface. This alignment of crystals is sometimes observed in crystallization under the presence of an solvent - air interface [73,74]. This theory is, to the authors best knowledge, not studied for ultrasound crystallization.

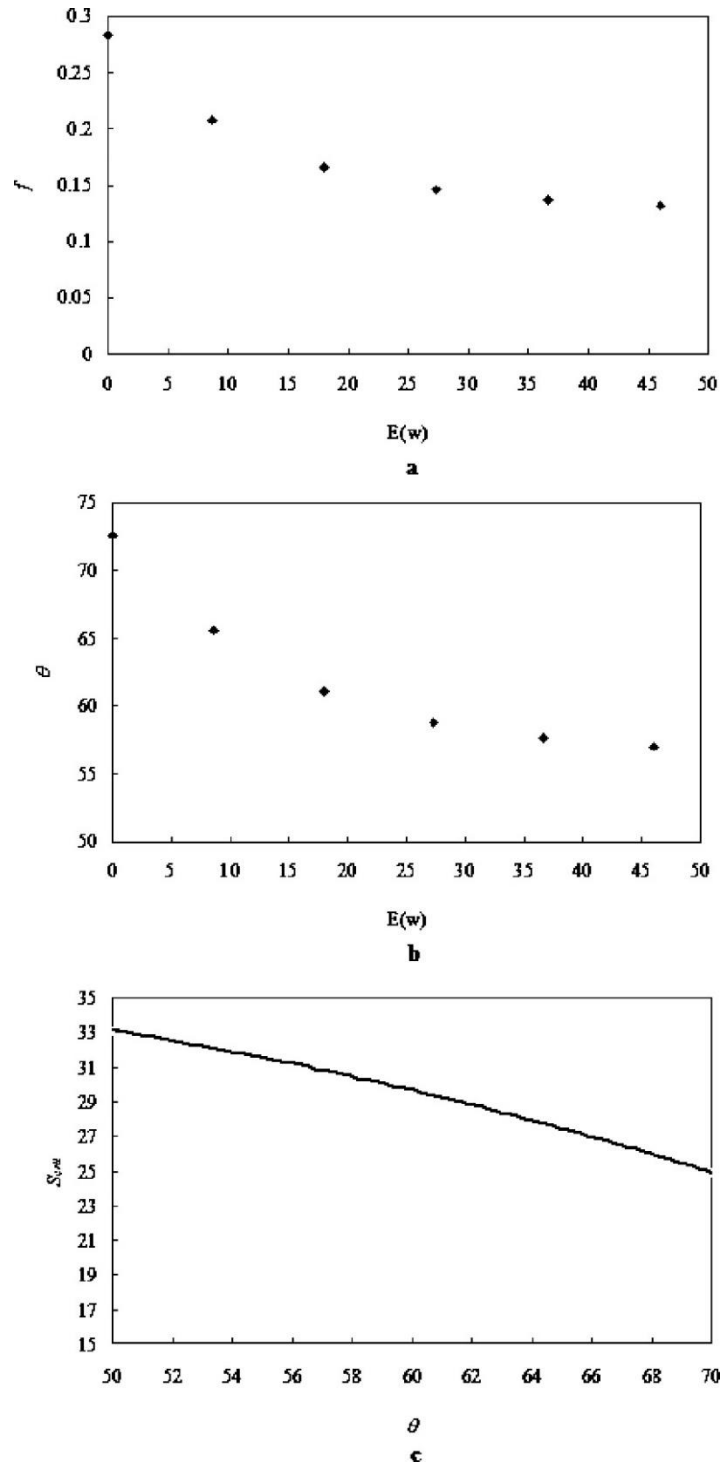


Figure 4. (a) The plots of geometric correction factor (f) vs ultrasonic energy input (E). (b) The plots of contact angle (θ) vs ultrasonic energy input (E). (c) The simulated relationship between critical supersaturation ratio (S_{crit}) and contact angle (θ). Reprinted from: Z. Guo; A. G. Jones; H. Hao; B. Patel; N. Li; Journal of Applied Physics 2007, 101, DOI: 10.1063/1.2472652, with the permission of AIP Publishing [32].

III Secondary nucleation

Ultrasound assisted secondary nucleation is believed to occur due to fragmentation of existing crystals upon implosion of the cavitation bubbles [46,75]. The fragments created upon fragmentation hence act as nucleation sites for new nuclei. Secondary nucleation is, as explained before, not well studied in literature and no articles were found which went in detail on the mechanism behind ultrasound assisted secondary nucleation. One can assume that the mechanism behind ultrasound assisted secondary nucleation is similar as the mechanism of ultrasound assisted particle breakage (i.e. sonofragmentation) which will be discussed later. [Ultrasound can create sonofragmentation in both supersaturated and undersaturated conditions.](#) [When this fragmentation occurs in a supersaturated solution, the fragments can act as nucleation sites for new nuclei. In this case, we speak about secondary nucleation. This formation of new nuclei does not happen always, in this case we talk about sonofragmentation.](#) A detailed study which proves that the mechanism is similar or which investigates the relation between the breakage and secondary nucleation rate upon sonication is, however, lacking.

One can conclude that for primary nucleation some doubts can be placed on the cooling, pressure, segregation and evaporation hypotheses. Experiments or calculations indicate that these hypotheses are not realistic. PIV experiments suggest that the flow induced nucleation hypothesis is realistic. On the contrary, gassing experiments of different components indicate that the hypothesis of the bubble as nucleation center seems reasonable to explain heterogeneous nucleation. The mechanism behind ultrasound assisted secondary nucleation is, to the authors' best knowledge, not yet investigated in detail.

2.2.Growth

The effects of ultrasound on crystal growth are less significant and therefore less clear than the ones on nucleation [3,76,77]. The most reported effects of ultrasound on crystal growth are related to the particle size and the shape of the particles.

2.2.1. Effects of ultrasound on particle size and particle size distribution

No consensus can be found in literature on the effects of ultrasound on the growth rate. In most cases no significant effects of ultrasound on the growth rate are observed because the effects are counteracted by the effects of ultrasound on fragmentation and nucleation [3,40,76]. Fragmentation results in particle size reductions, and ultrasound applied during nucleation can result in more initial nuclei which grow into smaller crystals in the end. Both effects counteract the possible larger crystals created by higher crystal growth rates upon sonication. In most cases, the effects of ultrasound on fragmentation and nucleation are larger than the ones on crystal growth so that smaller crystals are obtained in the end [3,40,76,78,79]. There are, however, a few papers which tried to investigate the effects of ultrasound on the crystal growth rate further.

Nii and Takayanagi reported the formation of larger glycine crystals during sonication with a 1.6 MHz transducer [80]. Crystals with an average size of 160 μm , instead of about 120 μm under silent conditions, and a narrower particle size distribution were obtained after 20 min sonication. The authors attributed this effect to the inclusion of microcrystals into growing crystals. This hypothesis was tested by sonicating a suspension of both fine and coarse glycine crystals in an anti-solvent (ethanol), effectively avoiding the nucleation step. Figure 5 shows some of the results of this study. The evolution of the average crystal size in time is given for different ultrasonic power levels. All curves show an increasing trend with time with the

strongest increase in particle size for the largest power settings. This means that faster crystal growth was obtained with increasing ultrasonic power levels.

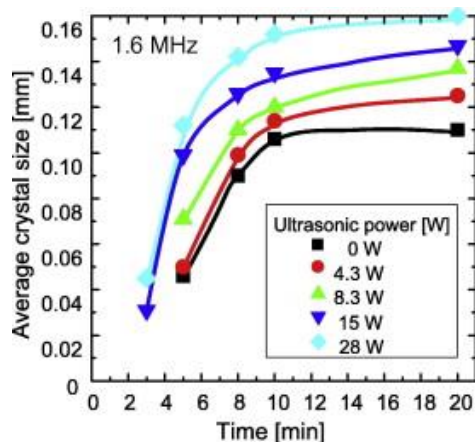


Figure 5 Change of crystal size in time for various ultrasonic powers at irradiation of 1.6 MHz. Reprinted from, *Ultrasonics Sonochemistry*, 21, Susumu Nii, Saki Takayanagi, Growth and size control in anti-solvent crystallization of glycine with high frequency ultrasound, 1182-1186, Copyright (2018), with permission from Elsevier [80].

Cao *et al.* studied evaporative crystallization of inorganic salts (NaCl, NH₄Cl) and proteins (lysozyme and proteinase K) in acoustically levitated droplets [68]. The sonicated droplets showed higher growth rates, larger final crystals and fewer crystals compared to a control vessel. The authors contributed these effects to acoustic streaming generated by a 20 kHz transducer. Acoustic streaming was thought to enhance the mass and heat transfer which promoted drop evaporation. This resulted in a faster increase of the supersaturation level and hence faster growth rates.

The effect of ultrasound irradiation on the crystal growth rate was also studied via simulations. Bari *et al.* performed gPROMS simulations of the growth kinetics of sonocrystallization of K₂SO₄ [40]. In this paper, they showed that ultrasound can increase the growth rate with 20%

compared to silent conditions. Ultrasound generates turbulences via acoustic streaming and via cavitation. These turbulences increase the mass transfer of molecules in the bulk liquid towards the growing crystal and could therefore enhance the crystal growth rate and thus result in larger crystals in the end. This effect was demonstrated by Rodchenkov and Sergeev during a single-crystal growth experiment of potassium dihydro-phosphate (KDP) [81]. Focused ultrasound of 1.4 MHz was applied to a solution containing one single crystal of KDP. This sonication resulted in 1.5 - 2 times higher crystal growth rates compared to free convection conditions. PIV experiments showed that crystal growth rates were maximum in the zones of the reactor where the flow rates were the highest. These results indicate that the enhanced mass flow rate could impact the crystal growth rate positively. This assumption of microturbulence-enhanced growth is also congruent with the fact that the strongest effects of crystal growth are observed at higher ultrasonic frequencies. Research in our group has shown, namely, that best micromixing was observed either at high ultrasonic frequencies around 1 MHz, where stable cavitation bubbles are formed, or at low ultrasonic frequencies around 20 kHz when transient cavitation bubbles are produced [82]. The latter frequency range showed, however, substantial sonofragmentation rates while the frequencies around 1 MHz did not induce any significant fragmentation [83].

This enhanced mass transfer has, however, only an effect on the growth rate when mass transfer is the rate limiting step during crystal growth. In most cases, surface nucleation and/or integration at the crystal faces determine the crystal growth rate [3]. At high supersaturation levels, a significant amount of possible growth units is available in the vicinity of the crystal surface. In that case, the rate limiting step in crystal growth is the surface nucleation and integration step rather than the mass transfer from the bulk to the crystal surface. Only at low supersaturation levels, this quantity of available growth units can become too small so that mass transfer becomes rate limiting in supplying growth units to the crystal surface. A theoretical

study indicated that at low supersaturation levels, the growth velocities are in the order of 10^{-10} m/s and ultrasound could enhance these rates with a factor 2. At high supersaturation levels, in contrast, growth velocities were in the order of 10^{-7} m/s and no effect of ultrasound on these growth rates could be observed [3]. Some authors state therefore that ultrasound can only impact the mass transfer and not surface nucleation or integration [84]. There are, however, to the authors' best knowledge, no publications published which investigated the effect of ultrasound on surface nucleation or integration during sonocrystallization.

Several articles report narrower particle size distributions when sonicating during the crystallization process [42,77,80,85–87]. This effect was observed both at low ultrasound frequencies of 20 kHz produced with an ultrasonic probe as with higher ultrasonic frequencies of 500 kHz and 647 kHz produced via a Langevin type multi-frequency transducer [85]. Bhangu *et al.* observed that the higher the applied power, the narrower the particle size distribution becomes [77]. Most articles explain these observations through the enhanced micromixing created via sonication [76,80,85]. Good micromixing ensures that the anti-solvent and temperatures are distributed well within the crystallizer so that local zones of high supersaturation are avoided. Hence, the crystals undergo more homogeneous growth and this results in smaller size distributions in the end. Another option is that ultrasound breaks agglomerates and hence creates a narrower distribution [40,83,88].

2.2.2. Effects of ultrasound on particle shape

Besides influencing the crystal size, ultrasound can also impact the crystal shape. Several articles and patents report the formation of more uniformly shaped particles under sonication [45,48,78,89–92]. Most of these papers report the creation of more spherical-like particles. Pohl *et al.*, for example, studied the precipitation of BaSO₄ nanoparticles in a continuous

sonochemical flow reactor [89]. The creation of spherical particles, compared to flat (flaky) particles under silent conditions, was observed by sonication at 20 kHz and 20-160 W. The reactor was a conical reaction chamber with a volume of 10 mL and a residence time between 4.5 - 15 s. More recently, Moghtada *et al.* created spherical CoTiO_3 nanocrystals during a low-temperature synthesis via sonication [78]. An ultrasonic bath with a frequency of 53 kHz and 500W power was used in these experiments. The shaping effect is not limited to nano-sized particles. For example, Byrne *et al.* created spherical particles in the micrometer range via sonication [92]. They investigated the ultrasound precipitation of manganese carbonate from aqueous solutions of NH_4HCO_3 and MnSO_4 . Again, spherical particles were produced by ultrasonic irradiation at 20 kHz and power of 400 W. Our research group investigated this ultrasound-induced shaping effect further [93,94]. Ultrasound was able to create spherical MnCO_3 particles at frequencies of 40 till 1135 kHz at both lab scale (190 mL) and semi pilot scale (50 L) as long as it was applied during the crystallization process. Sonication of precipitated particles, did not result in a change in particle shape [93]. Also other shape transformations, besides the creation of spherical particles, are reported during sonocrystallization. For instance, Li *et al.* reported shorter and thicker spectinomycin hydrochloride particles upon sonication compared to the needle-like crystal produced under silent conditions. Ultrasound was applied via a 15-30 kHz titanium probe with a maximum power of 1200 W [48].

Although the exact mechanism behind ultrasound shaping is still unknown, there are two commonly used theories reported in literature. The first one assigns the increased uniformity of the particles to the improvement in mass transfer rate between solution and surface [48,78,91,95]. Ultrasonic irradiation creates cavitation bubbles which collapse, resulting in microscopic turbulence and thinning of the hydrodynamic boundary layer around the particles. It is believed that these effects are responsible for an enhanced mass transfer in the mixture,

therefore increasing the possibility of the solute molecules to combine with each other and approach each side of the growing particle more uniformly and easily. This compensates the different growth rates at different crystal faces leading to more uniform crystals in the end. The second theory explains the formation of spherical particles by the melting of particles upon implosion of the cavitation bubbles [48,96–98]. Collapsing cavitation bubbles create intense shock waves which cause high velocity collisions of solid particles. These collisions result in extreme heating at the point of impact and as a result the particles are melted together [24]. The creation of agglomerates with smooth surfaces was observed during the sonication of Sn, Zn, Cu, Ni, Fe, and Cr slurries [7,24].

2.3.Polymorphism

Many organic and inorganic crystalline compounds display polymorphism. Polymorphs of a compound are basically different solid phases with identical chemical composition but different crystal structures. This results in a variation of chemical and physical properties such as dissolution rate, density, crystal shape etc. Many of these properties are crucial based on the application of the compound especially in case of pharmaceutical use. Due to these characteristics of polymorphism it becomes important to have better control on the crystal habit during crystallization processes of compounds.

Ultrasound has also the potential to produce crystals with a different polymorphic form compared to silent conditions [99–105]. This change in polymorphic form is, however, not observed in all papers in literature which investigated the effect of ultrasound on polymorphism [91,106,107]. The stability of the formed polymorph and the conditions under which ultrasound is applied seem to define whether a change in polymorph is observed or not [77,105,108]. Bhangu *et al.* investigated for example the ultrasound assisted crystallization of paracetamol

[77]. Under silent conditions, the most stable form of paracetamol, monoclinic (form I), was produced. Sonication at frequencies between 22 and 139 kHz resulted in the production of the less stable orthorhombic form (form II). This form II could, however, only be observed via microscope images obtained shortly after the crystallization experiment. Form II is metastable so that it transforms back to form I completely within 6 h even at 0 °C. Moreover, the supersaturation level at which the crystallization is performed has a major impact. Higher supersaturation levels favor nucleation of the comparatively more energetically less stable polymorph [77,105,108]. If supersaturation is low, and the nucleation rate is small, molecules clusters have sufficient time to re-orient and rearrange themselves during the nucleation stage so that a wide range of energy systems can be sampled. As a result, there is a high probability that finally the most stable form with the global energy minimum will be obtained [108]. At high supersaturation levels, in contrast, the molecule clusters have less time to reorient and rearrange themselves so that solution systems are likely to be trapped in a local energy minimum which could lead to the formation of a less stable polymorphic form. Ultrasound is thought to increase the rate of supersaturation formation so that the probability of creating the less stable polymorphic form increases [77,101,108].

The above-mentioned effects are observed over a wide frequency range of 20 kHz to 18.2 MHz. In the low frequency range, the effects of ultrasound are often explained by the creation of cavitation bubbles which can act as heterogeneous particles and create shear forces upon collapse in the liquid [77,101,102]. As a result, the nucleation rate is enhanced which can explain the formation of the less stable polymorphs. The effect of cavitation bubbles was specifically tested by Ike and Hirasawa during the antisolvent crystallization of *L*-ArgHCl [102]. Sonication via a 20 kHz probe resulted in at least 56.7% of the unstable β -form instead of 15.4% under silent conditions. This effect was independent on whether the solvent vessel or the antisolvent vessel was sonicated or if sonication was performed before or after addition of

the antisolvent. It was, for example, also visible when the antisolvent, where no L-ArgHCl was present, was sonicated and then transferred into the crystallization vessel. 60.6% β -form was obtained under these conditions. DLS measurements showed that the cavitation bubbles generated by the ultrasound stayed in the solution for at least several minutes and could be transferred into the crystallization vessel. It was thought that these bubbles impact the supersaturation of L-ArgHCl and therefore enhance the formation of the less stable β -form.

It is, however, likely that besides the cavitation bubbles also the enhanced turbulences and acoustic streaming generated by the ultrasound field play a role. Bai *et al.* observed for example that standing surface acoustic waves of frequencies between 6.0 and 18.2 MHz impact the polymorphic form of glycine [108]. **Sonication was provided via interdigital transducers which created surface acoustic waves induced streaming.** Sonication led to the formation of a higher amount of the less stable β -form of glycine compared to silent conditions. The higher the applied frequency, the higher the yield of the β -form. Sonication at 18.2MHz resulted for example in the formation of 91.3 % of the β -form compared to only 15.2 % under silent conditions. No cavitation bubbles are, however, generated at these high ultrasonic frequencies [11]. Acoustic streaming, which is more efficient at higher frequencies, is thought **to enhance the evaporation rate of the solvent (water) and** hence improve the rate of supersaturation generation [80,108]. As a result, the probability of formation of the less stable polymorphic form increases.

2.4.Chirality

Besides polymorphism, the application of ultrasound during the crystallization of chiral molecules (or achiral ones that form chiral crystals) has shown to impact the chirality of the product crystals, which is of high relevance to the pharmaceutical industry, as often only a

single enantiomer is desired. While the general consensus is that acoustic fields do not directly influence chirality and chiral crystallization, secondary effects arising from the cavitation process can greatly influence such a process. Chiral symmetry breaking during a sonocrystallization process is thought to occur mainly through ultrasound-enhanced secondary nucleation, where secondary nuclei originating from a parent crystal will retain the same chirality as the parent crystal, a phenomenon also observed during intense mixing and turbulence. In a biased (slight excess of one enantiomer) and/or competing system (through conversion of the enantiomers via racemization) this phenomenon may lead to chiral amplification [109–111].

An additional means to control chirality is the recently discovered Viedma ripening process, in which continuous fragmentation of a suspension of chiral conglomerate crystals in contact with their saturated solution leads to deracemization (evolution of the system from the racemic state to a single chirality), provided that chiral molecules racemize in the solution (or lose chiral identity, *e.g.* NaClO₃) [112,113]. Since ultrasound can cause substantial fragmentation of crystals in a suspension, our group recently investigated ultrasound as a potential means to replace mechanical grinding in Viedma ripening. The results revealed that sonofragmentation for NaClO₃ leads to abrasion resulting in the fast formation of many submicron fragments, as opposed to bead grinding that leads to fracture and relatively slower submicron particle formation. During sonication, these fragments readily dissolve in the nearly saturated solution leading to faster initial deracemization compared to the conventional bead grinding. However, deracemization was not complete due to the crystals reaching a constant uniform crystal size with several crystals of the counter enantiomer surviving. The intermittent addition of enantiopure seeds or the combination of ultrasound and bead grinding was shown to lead to complete enantiomeric purity in an accelerated manner. Rougeot et al. also investigated the application of ultrasound in the deracemization of a precursor to paclobutrazol (a plant growth

inhibitor). The application of ultrasound led to a faster deracemization compared to stirring in the presence of glass beads, while the deracemization rate increased with the applied ultrasound power [114].

The applications of ultrasound in chiral crystallization processes, such as diastereomeric resolution, preferential crystallization, total spontaneous resolution and deracemization is an emerging field and was recently thoroughly discussed by some of us elsewhere [115].

2.5.Fragmentation / deagglomeration

2.5.1. Observations on ultrasound assisted fragmentation / deagglomeration

Most research on sonofragmentation is performed on inorganic solids in water [35,57,85,116]. Raman and Abbas for example, studied particle breakage of aluminum oxide particles suspended in water under sonication with a 24 kHz probe [117]. The effects of ultrasonic powers of 150-350 W and temperatures of 10-50°C on breakage characteristics were investigated. The highest breakage rates were obtained within a temperature range of 25-37 °C and at the highest ultrasonic power. Temperatures below 25 °C or above 37 °C resulted in lower breakage rates. Two opposing effects were thought to explain this behavior. First the increase in cavitation events and hence an increase in breakage rates with an increase in temperature. Higher temperatures result in an increase in the vapor pressure and a decrease in the surface tension and viscosity, all of which result in a reduction in the cavitation threshold. Second, a cushioning effect of the cavitation intensity arises, which increases with higher temperatures. So higher temperatures lead to more bubbles but the impact of the bubble implosions is lowered

due to the cushioning effect. As a result, an optimum temperature exists where both effects are optimized to result in the highest breakage rate.

Recently, Kim and Suslick investigated the effect of the vapor pressure and viscosity during the sonofragmentation with a 20 kHz horn operating with a 2-second-on and 8-second-off pulse was used [118]. The effect of the vapor pressure was investigated by preparing slurries of potassium chloride in various organic liquids. No effect of the vapor pressure, ranging from 0.01 to 50 Torr on the fragmentation rate was observed. The authors concluded that the vapor pressure does not affect neither the total mechanical energy of the bubble before the collapse nor the bubble rebound that generates the shockwave launched into the liquid. In addition, potassium chloride solutions in dodecane and silicon oil were tested on the same setup. The viscosity of the solution is changed by the weight percent of silicon oil. As the viscosity of the solution increased, the fragmentation rate decreased and no significant breakage was observed above a viscosity of 100 cSt. Finally, also the effect of the Vickers hardness and Young's modulus on the sonofragmentation of six ionic crystals was investigated by the same authors. Table 1 shows the sonication time to halve the initial crystal size ($\tau_{1/2}$) for the investigated ionic crystals together with their Vickers hardness (H_v), Young's modulus (E) and initial crystal size. Longer sonication times were needed to reduce the initial crystal size to half with increasing Vickers hardness and Young's modulus. The fragmentation rate decreases monotonically with increasing Vickers hardness or Young's modulus. It was also demonstrated that the initial crystal size has no effect on the fragmentation rates of the alkali halides under the studied conditions. Jordens *et al.*, in contrast, observed that in some conditions crystal breakage occurs only till a certain minimum particle size [83]. Crystal breakage of paracetamol crystals in a saturated paracetamol-water solution was investigated under sonication with different ultrasound transducers and one probe. Sonication with a 97 kHz transducer at 20 W calorimetric power resulted in particle breakage for crystals with an initial size of 63-125 μm and 38-63 μm but

not for particles with a size below 38 μm . Sonication was applied for 180 min and no effect of ultrasound was observed on these smallest particles. Sonication with a 30 kHz probe at the same calorimetric power, in contrast, did result in particle breakage well below 38 μm . The main difference between both ultrasound sources was the type of cavitation bubbles produced. Stable bubbles were predominantly detected with the 97 kHz transducer while transient bubbles are most dominant with the 30 kHz probe. It was therefore suggested that the type of cavitation bubbles impact the sonofragmentation behavior. This was further investigated in the same study via Kapur function analysis. [Kapur function analysis uses a cumulative breakage distribution function to analyze the particle breakage \[27,119\]. The population balance models, which will be discussed in section 3, in contrast, use continuous breakage distribution functions. The main advantage of the Kapur function analysis lies in the simplicity of application to experimental results. This Kapur function analysis showed that stable cavitation bubbles mostly break via fracturing while relative more abrasion was present when transient bubbles were created. Using a similar setup to the previous study, Xiouras *et al.* also studied quantitatively the ultrasound breakage behavior of \$\text{NaClO}_3\$ particles suspended in the antisolvent hexane at a frequency of 41 kHz and 30W \(absorbed electrical power\) and compared the breakage behavior with that using bead grinding \[120\]. It was found that for the specific compound, ultrasound led to abrasion, generating many fine particles, while bead grinding caused mostly fracture of the crystals. Interestingly, a synergistic effect of bead and ultrasound grinding was observed when the two methods were combined, leading to higher breakage rates than the sum of the breakage rates attained using each method individually](#)

Table 1 Vickers hardness (H_v), Young's modulus (E), and sonication time necessary to halve the initial crystal size ($\tau_{1/2}$) of alkali halides. Copyright © 2017, John Wiley and Sons [118].

Alkali halide	H_v (GPa)	E (GPa)	$\tau_{1/2}$ (s)	Initial crystal size (μm)
NaF	0.626	77.5	900	500
LiCl	0.243	49.8	360	580
NaCl	0.216	37.3	310	340
NaBr	0.129	29.7	140	490
KCl	0.128	26.5	140	420
KBr	0.098	22.3	90	310

As a conclusion, one could state that sonofragmentation is impacted by the temperature, the Vickers hardness, the Young's modulus and the ultrasound source or type of cavitation bubbles. The initial crystal size, within certain ranges and dependent on the ultrasound source, and the vapor pressure have no impact on the breakage rate.

Besides fragmentation also deagglomeration of aggregates is observed under sonication [121,122]. Ivanov studied the ultrasonic treatment of Al-AlN, Al₂O₃ and AlOOH suspensions at 22 kHz and ultrasonic powers between 10 and 60 W [121]. The Al-AlN, Al₂O₃ and AlOOH aggregates, with sizes of 0.5 to 3.0 μm were destroyed upon sonication while the number of 0.2 to 0.5 μm particles increased significantly. Gielen *et al.* investigated the use of ultrasound for agglomeration control of an active pharmaceutical compound [123]. Ultrasound was evaluated both as a post-treatment technique to break agglomerates and as an alternative seeding agent. The former method proved to be unsuccessful since all crystals exhibited strong surface erosion and only part of the agglomerates could be destroyed. Sonication during the initial stage of crystallization, in contrast, was able to inhibit the formation of agglomerates as long as a sufficient exposure time was provided. Analysis with Focus Beam Reflectance Measurement (FBRM) and InfraRed (IR) tools identified that ultrasound should be enabled until the FBRM

and IR signal counts reach a steady state, corresponding to a complete desupersaturation of the solute at the seeding temperature. The ultrasonic treatment was thought to enhance the degree of micromixing, hence boost the amount of particles and increase the collision frequency. As a result, aggregates can be efficiently disrupted before they are cemented into agglomerates.

2.5.2. Mechanisms behind ultrasound assisted fragmentation / deagglomeration

The effects of ultrasound on sonofragmentation can be attributed to the implosions of cavitation bubbles. The implosions of both stable and transient bubbles create, among other effects, shockwaves, high pressures (order of 1000 bar), microjets and enhanced mixing [12,35,57]. Some research investigated in detail which of these effects contributed most to particle breakage. Different mechanisms for sonofragmentation are proposed in literature: interparticle collisions, particle-wall collisions, particle-probe collisions and particle-shockwave/microjet interactions. Zeiger and Suslick and Kim and Suslick demonstrated that, for organic molecules and ionic crystals, sonofragmentation occurs primarily via particle-shockwave interactions [57,118]. Aspirin crystals and ionic crystals were suspended in dodecane and irradiated with an ultrasonic horn at 20 kHz and 10 W. Interparticle collisions were excluded by studying the increase of the particle concentration in the slurry. The sonofragmentation rate was not significantly affected by the particle concentration as the particle size of potassium chloride crystals was reduced to 50 % of the original size after 140 s of sonication for all slurries ranging from 0.07 to 10 wt%. A similar observation was also made for aspirine particles in dodecane. Interparticle collisions were therefore not believed to contribute significantly to the sonofragmentation of crystals. Second, particle-wall and particle-probe decoupling experiments were conducted. A latex membrane was placed around, respectively, the potassium chloride

suspension and the ultrasonic probe as shown in Figure 6. No significant decrease in the fragmentation rate was, however, observed during these experiments compared to the experiment without the latex membrane. This was observed for both potassium chloride and aspirin. Therefore, the authors concluded that particle breakage of both ionic solids and organic molecules appear primarily due to the interaction of the solid particles with the shockwaves and microjets formed during cavitation.

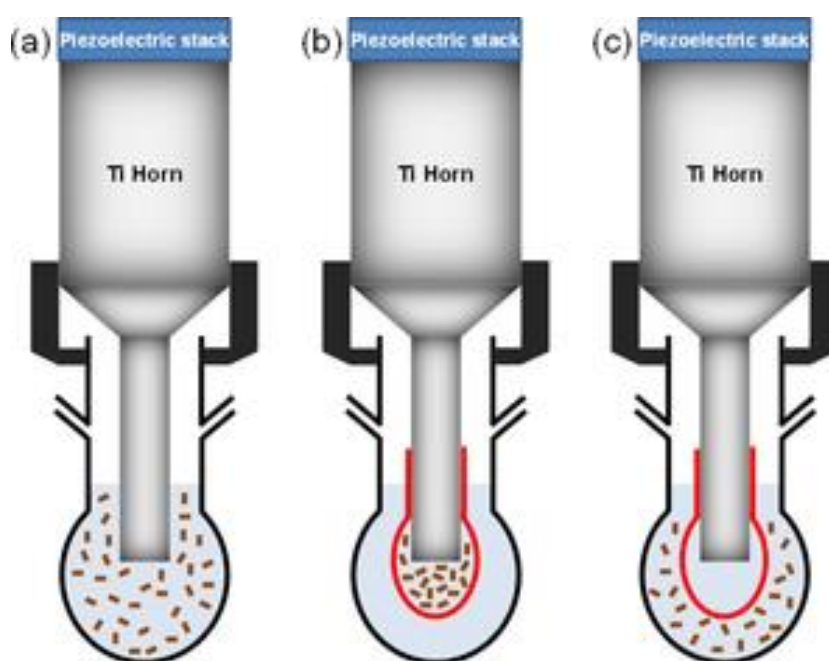


Figure 6 Experimental setups of (a) the normal apparatus showing the immersion of the titanium ultrasonic horn into the slurry, (b) decoupling experiments to eliminate particle–wall interactions, and (c) decoupling experiments to eliminate particle–horn interactions. Copyright © 2017, John Wiley and Sons [118].

Furthermore, Kim and Suslick suggest that it is likely that the morphology of the initial crystals defines the precise breaking mechanism [118]. High aspect ratio solids like rods, needles or plates are more likely to break through bending and torsion induced by the shockwaves or

microjets. Low aspect ratio solids, in contrast, will break through shock-induced compression-expansion.

Kudryashova and Vorozhtsov investigated the mechanism behind ultrasound deagglomeration of Al_2O_3 nanoparticle aggregates in an aluminum melt [122]. They suggested that the cavitation bubbles collapse near the agglomerates and hence create an overpressure which allows liquid to flow into the pores and overcome the capillary pressure. Melt is pushed in the capillary channels and, hence, the properties of the agglomerates are changed so that the separation of the aggregate into separate particles is facilitated when exposed to the ultrasound shockwaves or microjets.

3. Modelling of sonocrystallization and sonofragmentation

Population balance models (PBM) are well-established mathematical frameworks for simulating processes involving particulate entities, such as particle nucleation, growth, breakage and agglomeration. They can describe the evolution of the particle size distribution (PSD) during e.g. crystallization or fragmentation and thus they serve as valuable tools for the optimization and control of these processes. However, challenges in solving the resulting partial integro-differential equations, coupled with theoretical gaps in the understanding of the underlying phenomena in the presence of ultrasound (*e.g.* crystal growth or nucleation) have hindered their use to describe sonocrystallization. In the sections below, we discuss the few studies that have applied the PBM approach for simulating sonofragmentation and sonocrystallization processes. One of the main challenges faced in this field is to describe

nucleation and growth processes with physically-sensible parameters instead of adjustable model parameters.

3.1. Population balance modelling (PBM) for sonofragmentation processes

As discussed before, the exact mechanisms of sonofragmentation processes are still subject of ongoing scientific research, although it is generally believed that particle fragmentation occurs due to interactions of the particles with the cavitation bubbles formed in the liquid. According to the kinetic theory of grinding and neglecting other possible phenomena that affect the PSD, the change in PSD $n(v, t)$ (n in: # particles \cdot m⁻³ suspension volume \cdot m⁻³ particle volume, t in s and v in m³) for any perfectly mixed batch grinding process can be described by the population balance equation [124]:

$$\text{Eq. 5} \quad \frac{\partial n(v, t)}{\partial t} = \int_v^\infty \beta(v, v') S(v') n(v', t) dv' - S(v) n(v, t)$$

Where the first term on the right-hand side describes the death of particles of volume v' (m³) due to breakage. The second term describes the formation of particles of volume v (m³) due to breakage of v' size particles ($v' > v$). Functions $\beta(v, v')$ (m⁻³) and $S(v)$ (s⁻¹) are the probability of forming v sized particles from breakage of v' sized particles (daughter distribution function) and the breakage rate of particles of size v (breakage kernel), respectively. There are many theoretical and empirical daughter distribution functions and breakage kernels available in the literature and their choice is often reflective of the mechanism of the fragmentation process [125].

Kusters *et al.* were the first ones to apply the PBM (Eq. 5) for sonofragmentation processes [126]. Their model was validated via sonofragmentation experiments of agglomerated powders of silica and alumina dispersed in water. In their model, the authors assumed that the breakage

rate S is proportional to the number of collapsing cavities per unit time and inversely proportional to the suspension density. They also assume that the maximum radius of the collapsing cavities increases linearly with the square root of the ultrasonic power. Through these assumptions, they developed a general expression for the breakage kernel for a sonofragmentation process (Eq. 6):

$$\text{Eq. 6 } S(v) \sim \frac{kP^{1/2}v^{1/3}}{V_{tot}}$$

Where k is the ratio of ultrasound energy spent for cavitation to the total ultrasonic energy, P (W) is the ultrasonic power delivered to a suspension of volume V_{tot} (m^3). Following their experimental observations, the authors used a bimodal daughter distribution function to describe both erosion and fracture of primary particles that were detected experimentally. In addition, specific powder characteristics were considered in the daughter distribution function. The experimental PSD results (obtained by a sedigraph) were fitted to the model to derive the breakage rate parameters.

Rasche *et al.* also developed a PBM for the sonofragmentation of aspirin crystals suspended in dodecane [127]. In their study, they proposed a breakage kernel (Eq. 7) proportional to the ultrasound power P in watts and exponentially related to the dispersant fluid viscosity following their experimental results using dispersants of different viscosities.

$$\text{Eq. 7 } S(m) = S_0 P e^{-0.0069\eta} m^q$$

Where m is the mass (g) of the particle undergoing breakage, η is the liquid viscosity in cSt, S_0 is an efficiency factor and the exponent q is a positive constant. The kinetic parameters S_0 and q were estimated by comparing the experimental and model PSDs for different daughter distribution functions. For aspirin, the best fit was obtained for binary breakage (crystals break in half), which compared to the erosion-driven mechanism that was found in Kusters *et al.*

suggests that the breakage mechanisms are compound-specific and might be different for the often brittle organic crystals.

In a following study, Guillemin *et al.* studied the ultrasonic breakage of agglomerated ZnO nanoparticles suspended in water and developed a PBM to model the process [128]. Following the work of Kusters *et al.* the authors assumed a similar expression for the breakage kernel, but modified it to account for the mass of the agglomerates. Contrary to previous approaches, the authors converted the volume PSD (light scattering) that was measured experimentally to mass PSD by assuming size-dependent particle density of the agglomerates. Upon fitting the PBM to the experimental PSD, the authors could also correlate the measured calorimetric power generated in the medium rather than the electrical power to the breakage kernel by a square root law function.

Bari and Pandit, estimated the sonofragmentation kinetics of KNO₃ crystals suspended in toluene using a PBM [119]. In their model, a similar expression for the breakage kernel was used as the one developed in Kusters *et al.* The kinetic parameters were estimated based on fits of the experimental 0th moment of the PSD over different time intervals for several daughter distribution functions. A binary daughter distribution function (crystals break in half) was found to be more suitable to describe the observed evolution of the 0th moment.

3.2. Population balance modelling (PBM) for sonocrystallization processes

In a crystallization process, the PBM equation becomes considerably more complex, as the effects of crystal nucleation, growth and often agglomeration on the PSD must be considered together with breakage. Although the PBM is widely applied to conventional crystallization processes, only recently studies emerged where PBMs are also considered in sonocrystallization processes. Since the exact mechanisms of sononucleation are largely

unknown, most of the studies utilize the conventional expressions for the nucleation kinetics derived from the classical nucleation theory (CNT).

In most kinetic studies of sonocrystallization only nucleation and growth are considered, neglecting secondary phenomena such as breakage and agglomeration. Kim *et al.* were among the first to study the crystallization kinetics of the explosive 3-Nitro-1,2,4-triazol-5-one (NTO) experimentally and theoretically using ultrasound or mechanical mixing [129]. In their PBM, nucleation and growth were considered as simple power-laws and the difference between ultrasound and mechanical mixing was considered only by different pre-factors for the two phenomena. The orders for the two kinetic laws were kept constant. The pre-factor for nucleation was about 6 times higher for ultrasound versus mechanical mixing, while growth was similar for both phenomena. Narducci *et al.* also used a PBM with similar power laws for estimating the growth and secondary nucleation kinetics under the Mixed-Suspension Mixed-Product Removal (MSMPR) model, reaching to similar conclusions [130]. Comparable PBM models were developed in subsequent studies to model the antisolvent sonocrystallization of benzoic acid [76] and the seeded growth of (α) *L*-glutamic acid in the presence of ultrasound [131]. In the former study, application of ultrasound led to a higher nucleation rate constant and smaller particles, while in the latter, the growth rate constant was found to be slightly higher using ultrasound in the absence of nucleation.

A related approach was followed by Mateescu *et al.* for the sonocrystallization of calcium carbonate, but the authors also considered the crystal agglomeration process in their PBM [132]. By fitting the experimental PSD and concentration in the PBM to derive the kinetic parameters, they reported reduced agglomeration and increased nucleation and growth rate constants when ultrasound was applied. In a following study, Bari *et al.* developed a PBM model for the sonocrystallization kinetics of K_2SO_4 , considering all relevant phenomena, namely nucleation, growth, breakage and agglomeration [40]. In their model, total nucleation rate was considered

as the combination of primary and secondary nucleation, both of which were expressed in power laws. By fitting the experimental PSD, obtained by image analysis, and the concentration, the authors determined the rates of the relevant phenomena. By comparison of the estimated rate constants for sonicated and silent experiments, it was found that nucleation and breakage rates increased by the application of ultrasound, while growth rates were comparable for the two methods. In addition, agglomeration was found to be negligible in the sonicated experiments.

The first PBM study to consider sonocrystallization in terms of physical-based parameters was conducted by Kordylla *et al.* [133]. The authors proposed a PBM to simulate the cooling sonocrystallization of dodecanedioic acid from propyl acetate by introducing an additional kinetic expression for the nucleation process due to ultrasound irradiation. For the ultrasound initiated nucleation (by a short burst), a primary heterogeneous nucleation mechanism together with secondary nucleation was assumed, following the older theory of cavitation bubbles functioning as nucleation sites. The authors accounted for the change in nucleation mechanism using ultrasound by the reduction in the heterogeneous nucleation work due to a lower wetting angle θ between the cluster and the bubble surface area or due to the induced energy of ultrasonic waves. The latter would lead to a decrease in the activation energy and a subsequent decrease in the critical cluster radius. Their simulations, neglecting breakage and agglomeration, showed good qualitative agreement with the experimental PSD and concentration data. In a follow-up study, Wohlgemuth and Schembecker developed a more rigorous model including all relevant phenomena (nucleation, growth, breakage and agglomeration), for batch cooling crystallization, under induced nucleation, such as the application of ultrasound or gassing [134]. To account for induced nucleation, the authors used a similar approach as Kordylla *et al.*, using modified values of wetting angle θ and the interfacial tension. The crystal growth expression was also modified to account for

discrepancies between the experimental concentration and the model prediction. For the solution of the PBM, a sequential parameter estimation technique was developed and applied for different model systems.

In a later study, Bhoi and Sarkar developed a PBM for the batch unseeded cooling crystallization of L-asparagine monohydrate in water, considering nucleation, growth and breakage phenomena [135]. They considered overall nucleation rate as the sum of two terms: primary nucleation rate as expressed in CNT and an additional term for induced nucleation due to the ultrasound, which was described as a power law. For breakage due to the ultrasound, a binary (crystals break in half) daughter distribution was assumed and a breakage kernel in the form of a power law depending only on crystal size. The developed model showed a good agreement with experimental data of the concentration and mean crystal size.

4. Guidelines for operating parameters

With the current knowledge on ultrasound crystallization, a number of guidelines can be formulated with regards to operational conditions, with a view on industrial application of this technique. The operational parameters discussed are the ultrasonic frequency, type of cavitation bubbles, power, time window and moment of application. *It should be noted that other parameters such as reactor geometry, flow rate, impedance of the acoustic field in the reactor, external stirring etc. can also impact the acoustic field and cavitation behavior and hence influence the sonocrystallization process. These parameters are, however, not extensively studied in literature and are therefore not further discussed in this review.*

4.1. Ultrasonic frequency

The ultrasonic frequency has a significant impact on the nucleation, growth and fragmentation stages of the crystallization process. Figure 7 summarizes the optimal frequencies to maximize the impact on each of these stages according to Jordens [27]. Low ultrasonic frequencies are optimal to enhance nucleation and fragmentation rates. This optimal frequency range can be assumed to be generally valid as the same frequency range between 20 and 100 kHz is commonly reported as the optimal one for enhancement of nucleation and fragmentation in literature [3,10,48,77,136,137]. All these articles used different reactor designs and crystal types. Despite the fact that these articles report enhanced nucleation and fragmentation in this frequency range, the exact optimal frequency is probably reactor and system specific. Jordens *et al.* investigated, for example, the effect of frequencies of 16, 41, 98, 165, 570, 850 and 1140 kHz on the MZW in one single reactor geometry, at the same calorimetric power on one single product (Acetaminophen). The authors reported the highest reduction in MZW, and thus the fastest nucleation, at a frequency of 41 kHz [27,137]. Bhangu *et al.* investigated the antisolvent crystallization of the same component under similar ultrasonic frequencies of 22, 44, 98 and 139 kHz, but in a different crystallization vessel and in a mixture of ethanol-water instead of pure water. These authors observed the lowest induction times at 98 kHz instead of 44 kHz [77]. They speculated that, at 98 kHz, there was an optimum between the number of cavitation bubbles and the size of the bubbles. The size of the cavitation bubbles is inversely related to the applied frequency. One can make a rough assumption of the bubble size (R_{res}) based on the Minnaert equation: $R_{res} \approx 3/\text{frequency}$ [59]. A frequency of 16 kHz will result in bubbles with a size of 187 μm while at 165 kHz, the bubble size is only 18 μm and at 1140 kHz this size is further reduced to 2.6 μm . According to the different theories discussed in section 2.1.2, the larger the cavitation bubbles, the stronger the effect of cooling, pressure, evaporation, segregation, convection or heterogeneous nucleation. The number of cavitation events will

define the number of bubbles and one can expect that the more bubbles present, the more cavitation events occur and the faster nucleation becomes. The number of bubbles is, however, influenced by the number of antinodes present in the vessel which depends mainly on the applied frequency, the solvent and crystallization vessel design [12,77]. Therefore, one can expect that these factors will define the exact optimal frequency to enhance nucleation.

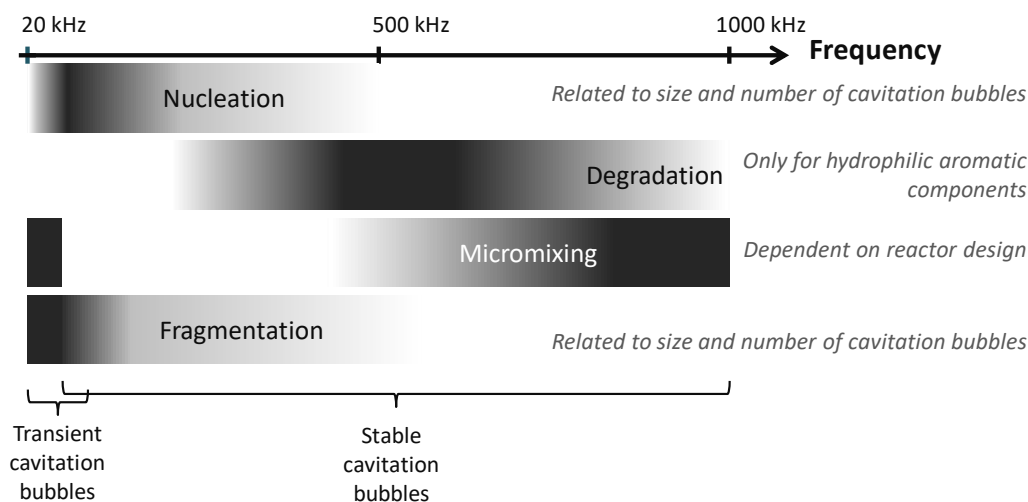


Figure 7 Overview of optimal frequencies for nucleation, degradation, micromixing and fragmentation. Dark colors indicate elevated nucleation, degradation, micromixing or fragmentation rates. © 2016 Jordens [27].

Similar observations were reported for sonofragmentation. Most articles report a significant particle size reduction with ultrasonic frequencies around 20 - 100 kHz while no or less size reduction is reported for significantly higher frequencies [48,80,83,85,136]. For example, Yamaguchi *et al.* reported significant breakage at 43 and 133 kHz while this was significantly less at 480 kHz [136]. Furthermore, Jordens *et al.* observed significant breakage of paracetamol crystals at 30, 41, 97 and 166 kHz while no significant particle size reductions could be seen at higher frequencies of 577, 850 or 1140 kHz [83]. These trends can be explained by the strength of the shockwaves created upon implosion of cavitation bubbles. Zeiger and Suslick already

showed that particle-shockwave interactions are the main source of particle breakage for molecular crystals [35]. Low ultrasonic frequencies will generate large cavitation bubbles which implode violently, hence generate strong shockwaves and therefore cause particle breakage [12,35,136]. High ultrasonic frequencies, in contrast, generate small bubbles which collapse less violently and hence generate weak shockwaves. Consequently, the degree of sonofragmentation will be low as well.

As discussed before, the effect of ultrasound on crystal growth is less pronounced than the effects on nucleation and fragmentation. To the authors' best knowledge, no effects of ultrasound on crystal growth are observed for low frequencies in the kHz range. These low frequencies are optimal for enhancing nucleation and fragmentation as discussed in the previous paragraphs. As a result, smaller crystals are obtained which could mask the possible positive effects of ultrasound on crystal growth in this frequency range. At higher frequencies close to the MHz range, in contrast, the effects on nucleation and fragmentation are negligible so that positive effects on crystal growth can be observed [80,138]. Nii *et al.* noted for example, significantly larger crystals during the antisolvent crystallization of glycine when sonicated with a 1.6 MHz transducer compared to silent conditions [80]. Sonication at 20 kHz, in contrast, created smaller crystals compared to silent conditions probably because of crystal breakage. The positive effects of ultrasound on crystal growth are thought to be created by the incorporation of microcrystals in the growing crystals or by the enhanced micromixing. The latter was found to be optimal at high frequencies close to the MHz range and stable cavitation bubbles or with transient bubbles generated at low frequencies [27,85,139,140].

Besides enhancements of nucleation, crystal growth and fragmentation, ultrasound has also potential to significantly impact the final crystal purity. Several papers in literature reported already the sonochemical degradation of organic compounds [137,141,142]. Degradation of pharmaceutical compounds can result in impurities which are detrimental to the final quality

attributes of pharmaceutical products. Ultrasonic degradation can be caused by pyrolytic degradation of the investigated compound or via $\bullet\text{OH}$ radicals and H_2O_2 formed by implosion of the cavitation bubbles. The route of degradation is dependent on the physical and chemical properties of the organic compound. Volatile aromatic components undergo mainly pyrolytic degradation, while aromatics with hydrophilic characteristics are degraded predominantly via the radical chain mechanism. The latter degrade mainly at intermediate frequencies between 165 and 850 kHz while the volatile aromatic components show higher degradation rates at low ultrasound frequencies (around 20 kHz) [137,143]. In addition, these volatile aromatic components can be removed from the solution due to evaporation in the degassing-bubbles created via sonication [144].

As a conclusion one can state that low ultrasonic frequencies in the range of 20 to 100 kHz create small particles, faster nucleation as well as crystal breakage, and these frequencies can be used to shape particles into more spherical-like particles. Higher frequencies around 1 MHz can be used to enhance micromixing and hence impact crystal growth when diffusion is the rate limiting step during the growth process. Intermediate frequencies of 200 to 800 kHz should be avoided when crystal purity is important and degradation of hydrophilic aromatic components can occur due to ultrasound.

4.2.Type of cavitation bubbles

Apart from the number and size of cavitation bubbles, some authors claim that also the type of cavitation bubbles influence the crystallization process. [As already explained before, two main types of cavitation bubbles exist, namely stable and transient bubbles \[12,54\]. The former live for hundreds of acoustic cycles \[55\]. As a result, gasses will be able to migrate through the](#)

bubble-liquid interface and enter the cavitation bubble or surface active solutes are able to adsorb on the bubble/solution interface and accumulate gaseous decomposition products [55]. These gas molecules and surface active solutes will absorb energy upon collapse and cushion the implosion. Transient bubbles, in contrast, expand very rapidly to at least double their initial size. These bubbles exist for only a short time, typically less than one acoustic cycle. Due to this short time frame, the dissolved gasses have insufficient time to cross the bubble-liquid interface and accumulate inside the bubble [145]. The resulting lack of gas cushioning causes transient bubbles to implode very violently. It is reported that the shockwaves and microjets caused by stable bubble implosions generate a lower pressure compared to transient ones [146–148]. As a result also the impact on the different stages of the crystallization process can differ between stable and transient cavitation.

The generated bubble type is determined by parameters such as host fluid properties, initial bubble size, acoustic pressure and acoustic frequency [149,150]. These factors are described in expressions for cavitation thresholds, like the Blake and Apfel thresholds [149–152]. In short, these expressions determine the pressure that the acoustic field needs to generate in order to produce transient bubbles. Additionally, these threshold values mark the transition between stable and transient cavitation. Further analysis of the equations shows that the threshold pressures can be more easily overcome at lower frequency, higher acoustic pressure and higher initial bubble size. This can also be seen in Figure 8 which indicates the zones of stable cavitation, transient cavitation and dissolving bubbles as function of the normalized bubble size (R) and acoustic pressure (P_a) [12].

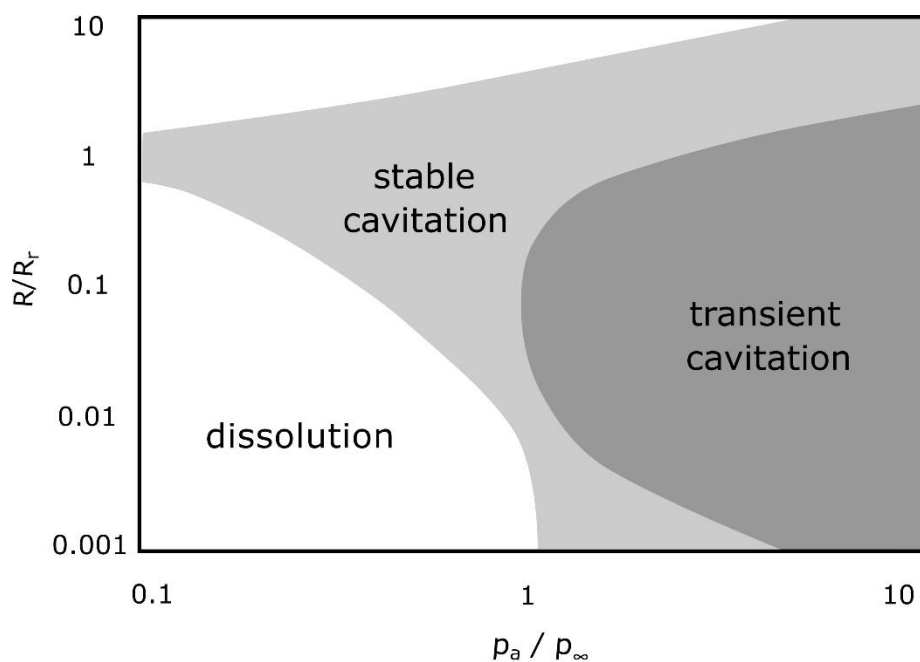


Figure 8 Regions of stable cavitation, transient cavitation and dissolving bubbles for a frequency of 20 kHz in water at ambient temperature and a static pressure (P_∞) of 1 bar. The acoustic pressure P_a is normalized by the bulk pressure (P_∞). Bubble radius R is normalized by the resonant bubble radius R_r . Reprinted with permission of, Copyright © 2019, John Wiley and Sons [12].

Jordens tested the effect of ultrasound from different ultrasound sources and different frequencies on the cooling crystallization of paracetamol [27]. The impact of sonication with an ultrasound probe operating at 30 kHz was compared with sonication via Bolt clamped Langevin transducers operating at 16 kHz, 41 kHz, 98 kHz and 165 kHz. All of these ultrasound sources were calibrated via calorimetry and the most dominant cavitation bubble type was determined via [multibubble sonoluminescence \(MBSL\)](#). The ultrasound probe was the only source which produced mostly transient bubbles [according to the MBSL technique](#). [The 16 kHz transducer generated visually detectable bubbles](#). However, [no sonoluminescence activity was observed at this frequency](#). These bubbles were therefore considered as sonoluminescent inactive bubbles. [The MBSL experiments in the same publication indicated that all other frequencies generated mostly stable cavitation bubbles](#) [27]. The effect of all these ultrasound sources was tested on the MZW of paracetamol [as can be seen in Figure 9](#).

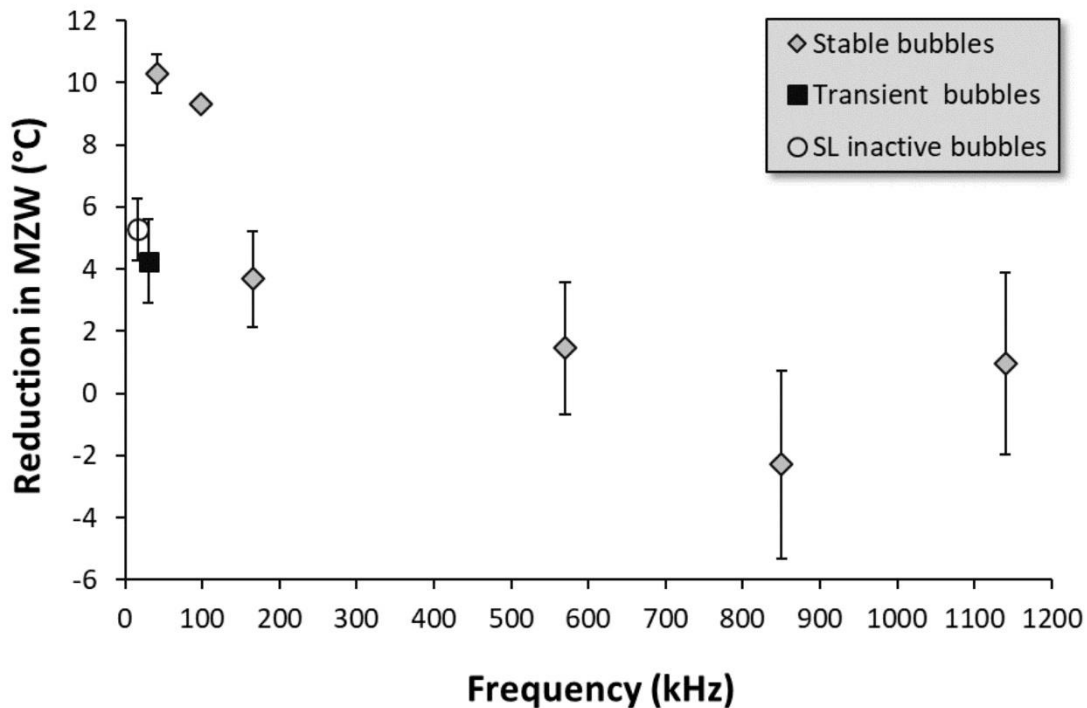


Figure 9 Reduction in MZW as function of the applied frequency for stable, transient and degassing bubbles. The error bars represent the standard deviation over 3 repetitions. © Jordens [27].

A significant reduction in the MZW of at least 4 °C was observed for all the tested frequencies. Moreover, the reduction in MZW was similar (3-5 °C) for SL inactive, stable or transient bubbles generated at 16 kHz, 165 kHz or 30 kHz respectively. These results indicate that the cavitation bubbles type has no major impact on the nucleation stage of the crystallization process. It is hypothesized, as discussed above, that the number and size of cavitation bubbles effect the nucleation rate.

A different trend is visible during sonofragmentation of particles, [as discussed before in section 2.5.1](#). Jordens *et al.* observed different breakage behaviors for transient and stable bubbles [83]. For transient cavitation bubbles, generated by a 30 kHz probe, higher specific breakage rates were obtained at higher ultrasound powers. This breakage rate was, however, independent of the applied power for stable bubbles generated via Bolt clamped Langevin transducers. Also

transient bubbles created relative more abrasion than stable bubbles which mainly caused particle breakage via fracturing. The highest breakage rates could be obtained by transient bubbles probably because these bubbles implode more violently so that the mechanical effects such as shockwaves, microjets and pressure waves are more violent compared to stable bubbles.

The effects of the cavitation bubble type on crystal growth are more difficult to study because of the strong crystal breakage, which interferes with crystal growth, by transient bubbles. No direct studies of the impact of the cavitation type on crystal growth were found in literature. The impact of the cavitation bubble type on the level of micromixing is, however, investigated in literature [139]. When considering that ultrasound impacts crystal growth by improving mass transfer, one would expect that improved micromixing results in better mass transfer and hence improved crystal growth. Best micromixing was observed for transient cavitation bubbles generated via a 30 kHz probe or stable bubbles from a 1140 kHz Bolt clamped Langevin transducer [139]. As discussed before, sonofragmentation will be more severe for transient bubbles compared to stable ones so that the effects on crystal growth will be only marginal. This was observed by Gielen *et al.* during the sonoprecipitation of MnCO_3 by two ultrasound probes and one Bolt clamped Langevin transducer [153]. The ultrasound setup was the same as in the article where micromixing was investigated so that transient bubbles could be expected for the ultrasound probe and stable bubbles for the ultrasound transducer [139]. The ultrasound transducer, operated at 40 kHz, created spherical particles with high tapped densities of 2.07 g/cm^3 . The ultrasound probes operated at 30 kHz and 36 kHz created more irregular shaped MnCO_3 particles and hence lower tapped densities of 1.79 g/cm^3 and 1.95 g/cm^3 respectively. These differences are probably caused because the probes generated transient bubbles, which collapse more violently and hence create more crystal breakage. The ultrasound transducer, [in contrast to these probes](#), generates mostly stable bubbles which create less

particle breakage so that the beneficial effects of ultrasound on the particle shape become more visible.

It is believed that always a combination of stable and transient bubbles is present but that one of them is more dominant [154,155]. Stable bubbles are mostly observed with plate transducers or Langevin transducers while transient bubbles are typically observed with ultrasound probes [56,83,139,155]. However, differences in frequency, position of the ultrasound source, reactor design, ultrasound emitter area and ultrasound intensity could influence the ultrasound field and hence impact the cavitation bubble type. Tronson *et al.* observed transient bubbles with a probe operating at ultrasound intensities of 0.1-0.4 W/cm² and stable bubbles with a 515 kHz plate transducer operating in a similar intensity range of 0.04-0.4 W/cm² [56]. These results indicate that the ultrasound intensity is not the most defining factor for the cavitation bubble type as both bubble types are observed in the same ultrasound intensity range. The authors thought that the differences in frequency could explain the different bubble types. However, Ashokumar *et al.* showed dependency of the cavitation bubble type on the ultrasound source rather than the frequency [155]. A 25/37 kHz transducer produced stable bubbles while a 20 kHz probe generated transient bubbles. This indicates that low frequency ultrasound, with frequencies below 50 kHz, is able to produce stable cavitation bubbles when transducers are used as the ultrasound source [154,155]. Ashokumar *et al.* suggested that the standing wave fraction of the acoustic field determines the degree of stable cavitation [155]. Traveling waves are thought to make the bubbles more shape-unstable which makes their behavior more transient. Standing waves, in contrast, do not create this shape distortion and promote therefore the existence of stable bubbles. It was also suggested that at high ultrasonic frequencies the acoustic field is predominantly a traveling wave [156]. This hypothesis was investigated by Ashokkumar *et al.* by placing a thin parafilm on top of the liquid surface [155]. This film reduces surface vibrations and promoted therefore the creation of standing waves. Sonication was performed by a 25 kHz

plate transducer and the degree of stable cavitation increased significantly when the thin parafilm was used compared to the same transducer without the film.

Apart from the ultrasound source, also the flow rate of the liquid medium has an impact on the cavitation bubble type. Gielen *et al.* investigated the effect of flow rate on the type of cavitation bubbles in a milliflow ultrasound reactor at frequencies of 45 kHz, 119 kHz, 247 kHz and 564 kHz [154]. Stable bubbles were observed, regardless of the flow rate, at 247 kHz and 564 kHz. At 45 kHz and 119 kHz, however, mostly transient bubbles were observed at Reynolds numbers below 2300. At these flow rates, the flow can be defined as laminar. At flow rates above 2300, the flow regime shifts to turbulent flow and stable cavitation bubbles were observed under these conditions. These results indicate that the type of cavitation bubbles is also influenced by the flow regime, e.g. laminar or turbulent.

4.3. Ultrasonic power / pulse duration

A reduction in MZW or induction time with an increase in ultrasonic power is commonly reported in literature [32,75,86,87,157,158]. Higher ultrasonic powers create more cavitation clouds which lead to higher primary and secondary nucleation rates. As a result, more nuclei are generated which eventually grow into smaller particles [42,86,157]. This is in agreement with the proposed hypotheses on the effect of ultrasound on nucleation which were discussed above. However, the research group of Izumi Hirasawa published several papers which state that, at low supersaturation levels, a critical energy level E_{crit} (J) exists for crystal nucleation [159–161]. This critical energy level is defined as the ultrasound energy at which the induction time switches from high to low relative to the induction time without ultrasound irradiation [159]. At ultrasonic energy levels below this critical level, nucleation is inhibited so that a lower

number of nuclei is produced and the induction time is increased. At ultrasonic energy levels above this critical energy level, in contrast, nucleation is promoted, hence more nuclei are produced which result in a decrease in induction time compared to silent conditions. This hypothesis was tested on the cooling crystallization of *L*-Arginine, *L*-Serine and acetylsalicylic acid [159–161]. The value of the critical energy level is proportional with the critical free energy for nucleation (energy needed to form a stable nucleus) ΔG_{crit} (J) and therefore depends on the supersaturation level, the temperature, the solvent and the component. For acetylsalicylic acid, the critical energy level was between 120 and 200 J depending of the supersaturation level [161]. For paracetamol, in contrast, this critical energy level was estimated to be 500 J [162]. The relation between the critical energy level (E_{crit}) and ΔG_{crit} is given by Eq. 8 [161].

$$\text{Eq. 8 } E_{crit} = 2.0 \times 10^{20} \Delta G_{crit} - 69$$

These zones of nucleation inhibition and promotion are shown in Figure 10.

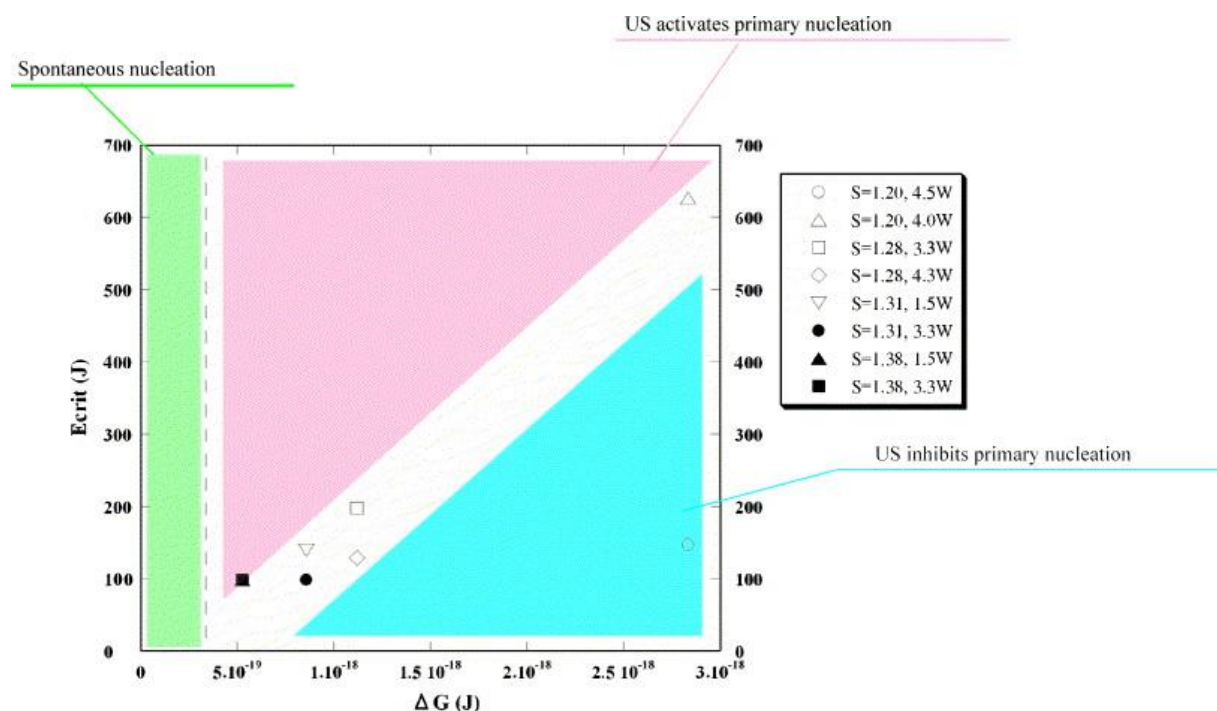


Figure 10 Critical energy level in function of the minimum free energy for nucleation. The red zone indicates where ultrasound activates nucleation, the blue zone where ultrasound inhibits primary nucleation. In the green region, spontaneous nucleation occurs. Reprinted from *Journal of Crystal Growth*, 295, Etsuko Miyasaka, Satomi Ebihara, Izumi Hirasawa, Investigation of primary nucleation phenomena of acetylsalicylic acid crystals induced by ultrasonic irradiation—ultrasonic energy needed to activate primary nucleation,97-101, Copyright (2018), with permission from Elsevier [161].

This critical energy level was only observed for low supersaturation levels of 1.20 and 1.28. At higher supersaturation levels of 1.31 and 1.38, sonication did not inhibit crystal nucleation. It is thought that at low supersaturation levels, subcritical clusters are only formed in certain regions in the liquid where there is locally a higher degree of supersaturation. When ultrasound is applied, violent ultrasonic streaming is generated which disperses the subcritical clusters and therefore inhibits nucleation. At higher supersaturation levels, these subcritical clusters are more abundantly available in the liquid and therefore hardly dispersed by the ultrasonic irradiation. These subcritical clusters become therefore more stable and form critical nuclei which crystallize [161].

Several articles report also increased effects of ultrasound on fragmentation and crystal growth at higher power levels compared to lower power ultrasound irradiation. An inverse relation between the particle size and the applied power is observed in several papers which studied the effect of ultrasound on particle breakage [16,117,136,163]. Raman and Abbas, for example, studied particle breakage of aluminum oxide particles suspended in water under sonication with a 24 kHz probe [117]. The effects of ultrasonic powers between 150 and 350 W on breakage characteristics were investigated. Sonication with 350 W resulted in a 17 % reduction in particle size after 5 min, compared to only ca. 13 % size reduction at 150 W in the same time span. As

explained above, higher power levels create more and larger cavitation bubbles which collapse more violently and hence generate stronger shockwaves, microjets and turbulences which eventually will create particle breakage. Jordens *et al.* observed that the power effect of ultrasound can also depend on the type of cavitation bubbles [83]. Sonofragmentation of paracetamol crystals in a saturated water solution was investigated for an ultrasonic probe and plate transducers. Stable cavitation bubbles created by a 41 kHz plate transducer caused similar particle size reductions for sonication at 10 W, 20 W or 30 W during 180 min of sonication. The sonofragmentation caused by transient bubbles, generated by a 30 kHz probe, in contrast, was dependent on the applied power. Sonication at 30 W resulted in 30 % smaller crystals after 180 min of sonication compared to sonication at 10 W. As discussed before, Kapur function analysis showed that the stable bubbles caused particle breakage predominantly via fracturing independent of the applied ultrasound power. For transient cavitation bubbles, in contrast, relatively more abrasion was detected at higher power levels.

Also for crystal growth similar observations are reported. Nii and Takayanagi studied the crystal size during the anti-solvent crystallization of glycine at 1.6 MHz [80]. Larger crystals were observed after sonication compared to silent conditions which was attributed to enhanced crystal growth. The larger the applied power, the larger the final crystal obtained. Sonication at 28 W resulted in crystals with an average crystal size of about 160 μm after 20 min of sonication. At a power level of 4.3 W, crystals of only 120 μm were obtained.

Ultrasound power and pulse rate affect in some cases also polymorph selectivity in a crystallization process. Gracin *et al.* investigated the effect of ultrasound on the polymorph habit in the cooling crystallization of p-Aminobenzoic acid (PABA) [104]. PABA has two polymorphic forms: the α - form and the β - form. In experiments without ultrasound by Gracin *et al.* the β - form was very difficult to nucleate even under the transition temperature of 25 °C

[164]. β - form crystallized only at a temperature of 13 °C at a supersaturation of 1.5. With ultrasound, β - form crystallized at much higher temperatures and even up to 8 °C above the transition temperature. In their work pulsed ultrasound was applied to avoid excessive temperature rise from ultrasound. Keeping the ultrasound frequency and pulse duration constant at 20 kHz and 1 s. they varied the ultrasound intensity (W/cm^2) by varying the applied power and gap time between pulses. In one set of experiments the ultrasound intensity was increased from 1.3 to 10.1 W/cm^2 by a combination of power increase and gap time decrease. The crystallization temperature in these experiments was close to the mentioned transition temperature of 25 °C. They found that below ultrasound intensity of 2.6 W/cm^2 , either a pure β form crystallized or a concomitant mixture of β and α . At higher ultrasound intensities it was always the α form. In the second set of experiments, where crystallization temperature was above the transition temperature, the ultrasound intensity was varied purely by reducing the gap time between ultrasound pulses. The ultrasound intensities were in the range of 2.1 to 10.1 W/cm^2 . The gap time between pulses was reduced from 9 s to 1 s. In these cases they observed always polymorph β at intensities below 3.4 W/cm^2 . The authors consider two possible reasons for ultrasound favoring formation of the metastable β form. First, high temperature and pressure of cavitation possibly disrupting the dimerization of the centro symmetric carboxylic acid which supports the formation of the α structure. Second is the disruption of such dimerization due to the electric field around a cavitation bubble. However, the reason for low power ultrasound to support the metastable polymorph was not understood.

In a work by Parimaladevi *et al.* pulsed ultrasound was used to control the polymorph of Vanillin in evaporative crystallization [165]. The solution was sonicated at varying power, pulse rate and total sonication time at a constant frequency of 20 kHz. Pulse rates of 10%, 30% and 50%, described in percentage of the total sonication time, were tested. For each pulse rate, experiments were carried out for five different sonication times from 1 to 5 min in 1 min steps.

Experiments were also carried out at 5 different power settings from 10 – 30 % of 750 W in steps of 5% for each combination of pulse rate and sonication time. Vanillin has four different polymorphs in which form I is the stable form and form II is metastable. Form III and IV are very rare. They found that ultrasound induces the nucleation of the metastable form II concomitantly with form I. They noticed at low pulse rate of 10 %, higher sonication times (3 – 5 min) and higher powers (20 to 30 % of 750 W) favor the nucleation of the metastable polymorph form II (concomitantly with form I). At medium pulse rate of 30 % all powers and sonication times nucleated as well form II concomitantly. However, at even higher pulse rate of 50 %, form II did not nucleate for higher sonication times of 3 – 5 min. For their experiments, medium exposure to ultrasound seemed to promote nucleation of form II. At higher powers of ultrasound a characteristic problem of ‘liquid-liquid phase separation’ with Vanillin hinders the nucleation of form II.

Ike *et al.* investigated the effect of ultrasound on the polymorph selectivity of L-Phenylalanine (L-Phe) in a cooling crystallization procedure [103]. L-Phe has two distinct crystal forms, anhydrate and monohydrate. Cooling crystallization was carried out at two different temperatures of 313 K and 293 K starting from a temperature of 353 K. An ultrasonic horn working at 20 kHz was used in their study. For crystallization experiments at 293 K, where the monohydrate form was stable, ultrasound always nucleated the stable form. Three ultrasonic powers were tested, namely 0.055 W, 1.4 W and 3.0 W. In all conditions, the monohydrate form was crystallized with improved yield in comparison to the experiments without ultrasound. They noticed here that US powers higher than 3 W caused temperature rise of more than 3 K which could possible influence nucleation. For the experiments at 313 K, the anhydrate form was the most stable at that temperature. Here they found that the monohydrate form nucleated in the experiments without ultrasound. At higher power of 3 W, ultrasound also promoted nucleation of monohydrate. However, at low powers the yield of anhydrate form was

much higher than the monohydrate form. Therefore ultrasound seems to support the nucleation of the stable polymorph at low powers.

It appears from the above mentioned literature that the effect of power and pulse rate on polymorph selectivity seems to be subjective to the compound. For the case of PABA higher powers favored formation of the stable polymorph but for L-Phe higher powers favored the metastable monohydrate. In case of Vanillin, relatively medium powers seemed to support the formation of the metastable polymorph. But one cannot be sure in case of Vanillin because of other effects that interfered in the nucleation process. However, all three works emphasize on the use of either pulsed or low power ultrasound to avoid the practical problem of temperature rise that could affect the supersaturation and in turn the polymorph.

Several articles report higher degradation rates of organic components with increased ultrasound power levels [141,142,166,167]. Higher ultrasound power levels are thought to generate more active cavitation bubbles which hence increase the amount of radicals formed. As these radicals can degrade organic components, as discussed before, one can expect that increased ultrasound power levels can result in more impurities which impact the crystal purity.

4.4. Time window

Dhumal *et al.* reported that higher sonication intensity and longer sonication time yielded the smallest crystals below 2 μm with a narrow size distribution during an antisolvent crystallization of salbutamol sulphate particles [6]. Kim *et al.* showed that a combination of in-line ultrasonic treatment at 20 kHz, and a subsequent temperature cycling protocol improved particle uniformity and modified the crystal shape of a Bristol-Myers Squibb drug substance

[168]. Li *et al.* also stated that proper adjustment of the power density and ultrasonic treatment time provides control over the final size distribution of the crystals. They reported an inversely proportional dependence of the particle size on the sonication time and a non-linear correlation with the power density, allowing to alter the average particle size of 7-ACDA within a range of 10-30 μm [95]. Moreover, intense research on the ultrasonic crystallization of adipic acid concluded that ultrasound produces particle sizes comparable to micronization, with an even narrower size distribution [169]. In addition, it was shown that a short ultrasonic burst in the beginning of the cooling cycle yields a comparable particle size and shape as the conventional seeding process [170]. The approach of ultrasonic seeding with different exposure times and power levels was also investigated in the reactive crystallization process of cloxacillin benzathine. It was concluded that the produced needle crystals were smaller and showed less agglomeration when a longer sonication period and a higher power was used. Also, a short burst in the beginning of the crystallization, which generated in-situ seeds, was already sufficient to produce more regularly shaped particles. Prolonged exposure to ultrasound further facilitated the control of the particle morphology and size distribution [171]. In general, it is believed that the crystal properties can be controlled by altering the ultrasonic exposure time and power [172,173].

In spite of these promising results, the additional energy requirement of ultrasound often inhibits scale up and industrial application [8,174]. An interesting approach to solve this restriction is the application of pulsed ultrasound that reduces the energy demand by periodically turning the sound field on and off [173,175–177]. Moreover, previous studies showed that the cavitation activity can even be enhanced compared to continuous sonication by adequate control of the pulse-on and -off time [149,178,179]. This was successfully applied during ultrasonic crystallization of glycine by Louisnard *et al.* By providing a correct setting of

the pulsation, they could even obtain faster nucleation kinetics compared to continuous exposure [180]. Pulsed ultrasound was also used to study the primary and secondary nucleation of ice crystals from water with various sucrose concentration. Using a duty cycle (DC) of 10% and 50% at various power levels, an improvement in nucleation temperature was obtained compared to non-sonicated conditions. Results show that higher power levels and longer pulse lengths, *i.e.* higher DC, yield more nucleation. However, the nucleation temperature tends to level off above a certain threshold power [44,158]. This was also observed during a recent study of Gielen *et al.* on the effect of pulsed ultrasound on the cooling crystallization of paracetamol [162]. Pulsed ultrasound with varying DC was applied to both a batch crystallizer and recycling flow crystallizer. Similar nucleation temperatures and particle sizes, compared to continuous sonication, were observed in both setups when ultrasound was switched on more than 10% of the time (DC of at least 10%). At DC of less than 10%, the nucleation temperature dropped significantly as can be observed in Figure 11. In addition, the median particle size increased more than 70% when the DC was decreased from 10% to 0%. The authors postulate that these optimal pulse settings of 10% DC correlate to the bubble dissolution time. During the pulse-on time, cavitation bubbles are formed. These bubbles will start to dissolve during the pulse-off time. When the optimal pulse settings are applied, the pulse-off time should be just long enough to avoid complete dissolution of these bubbles. Gielen *et al.* calculated that, for their specific reaction conditions, the bubble dissolution time was in the range between 1.3 and 1.9 s which corresponds to a DC range of 9.3-13.2% [162]. The experimentally observed optimal DC of 10% falls exactly within this range.

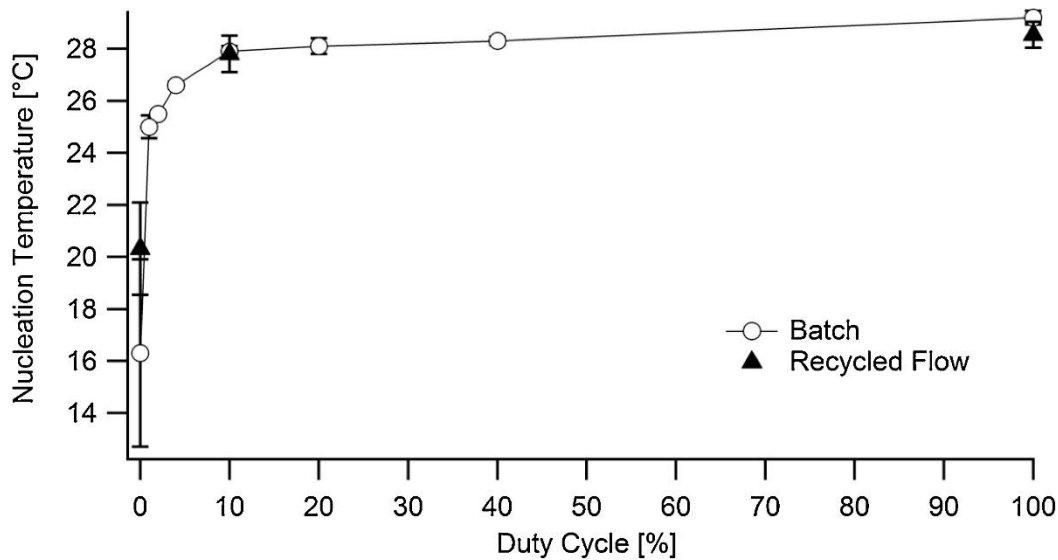


Figure 11 Effect of different ultrasonic duty cycles on nucleation temperature of paracetamol for the batch and recycled flow crystallizer. Reprinted from Chemical Engineering and Processing, 114, Bjorn Gielen, Piet Kusters, Jeroen Jordens, Leen C.J. Thomassen, Tom Van Gerven, Leen Braeken, Energy efficient crystallization of paracetamol using pulsed ultrasound, 55-66, Copyright (2018), with permission from Elsevier [162].

These results indicate that the energy consumption can be often reduced significantly via pulsed ultrasound while still similar crystal properties can be achieved as under continuous irradiation.

The sonication time impacts, just like the power, the amount of radicals formed. The longer the sonication time, the more radicals are formed and the more degradation of organic components occurs [141,142,166,167]. If one translated these results to the purity of crystals, this would mean that longer sonication times could result in more impurities.

4.5.Moment of application of ultrasound

In most studies on ultrasonic crystallization, sonication is enabled for a fixed time interval during or after a certain supersaturation level is induced by cooling or antisolvent addition [6,10,95,169,170,181–184]. However, the moment when ultrasound is applied in the process can also influence the final crystal properties as demonstrated by Park *et al* [157]. For this study, antisolvent crystallization of roxithromycin was used as a model system. This compound was dissolved in acetone at various concentrations, followed by addition to an aqueous solution to induce supersaturation and particle formation. To evaluate the effect when ultrasound is applied, a fixed sonication period of 5 or 20 s was imposed on the system when a certain time interval (10 – 150 s) had passed after mixing of the organic solution and the antisolvent. In all these experiments, the total time for crystal growth was maintained constant at 10 min and the average particle size of the crystals was determined. The use of ultrasound reduces the particle size primarily when it is applied in the initial stage of the crystallization, *e.g.* within a short period after mixing of the organic solution and the antisolvent. The authors report that in this initial phase nuclei are formed and crystal growth starts. Application of ultrasound in this stage affects the particle formation mechanism and induces collision-induced secondary nucleation, reducing the average particle size. In case the ultrasonic treatment is prolonged till about 120 s after mixing, a similar particle size is obtained as in the absence of ultrasound since nucleation and growth were already completed [157].

Later on, the group of Kim *et al.* used the same methodology, as discussed above, to study the effect of the moment when ultrasound is applied during antisolvent crystallization of griseofulvin [185]. Similar as for roxithromycin, ultrasonic waves only caused a reduction in the particle size when they were applied in the initial stage of the antisolvent crystallization process, *e.g.* the mixing step. Sonication when about 120 s had passed after mixing did not show any significant effects on the reduction of the particle size, as secondary nucleation can no

longer be promoted by the ultrasonic waves. It should, however, be noted that ultrasound was only applied for a very short time of 5 to 20 s and that significantly longer sonication times can still result in crystal breakage and thus the production of smaller particles.

Hatkar *et al.* studied antisolvent crystallization of salicylic acid in the presence of ultrasound and also briefly discussed the effect of time of application of ultrasound [186]. Sonication was enabled after various periods since the moment of addition of the organic solution to the antisolvent. Similarly to the previous works, it was reported that agglomeration only reduced if ultrasound was applied within 2 min after this addition step.

Another study on the use of [high intensity ultrasound \(HIU\)](#), [applied by an ultrasonic probe](#), during crystallization of interesterified soybean oil also investigated if the time when sonication is applied affects the properties of the crystals [187–189]. Therefore, a comparison was made between experiments in which: (i) no ultrasound was applied (wo HIU), (ii) HIU was activated before crystals were present (HIU @ T_c), and (iii) when the first crystals were observed (HIU @ f_c). These tests were evaluated at two different temperatures, corresponding to different supersaturation levels, using a constant ultrasonic power of 101 W. Figure 12 shows the obtained microstructure of the crystals for the various experimental conditions. These images demonstrate that HIU causes a more significant particle size reduction when it is applied in the presence of crystals. Based on these results, the authors concluded that the effect of HIU on secondary nucleation is larger than its effect on primary nucleation. Consequently, it was suggested that application of HIU in the presence of crystals is the most effective way to minimize the crystal size.

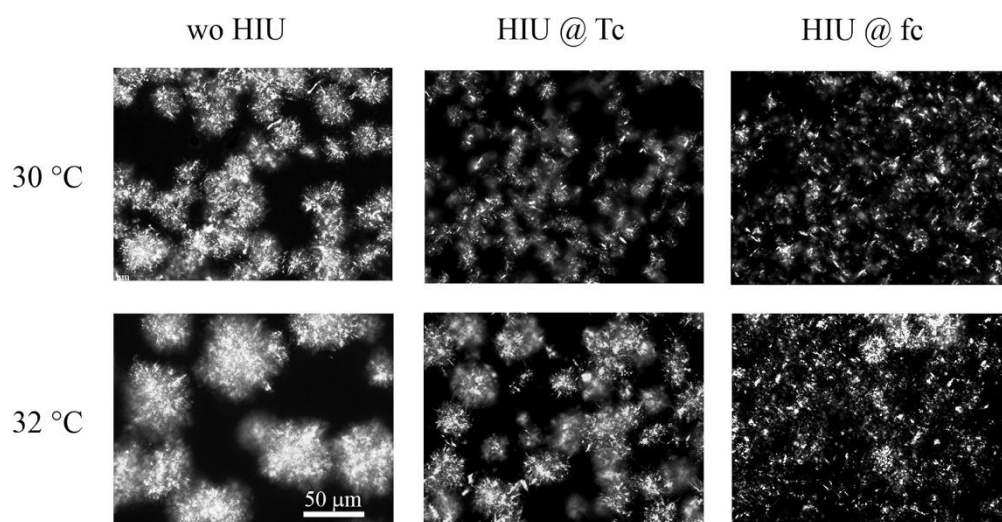


Figure 12: Interesterified soybean crystals obtained after application of HIU (101 W) at different moments in the crystallization process. Experiments were performed at two different supersaturation levels (30 °C and 32 °C). wo HIU: no ultrasound applied, HIU @ T_c: sonication in the absence of crystals, HIU @ f_c: sonication after the first detection of crystals. Reprinted with permission from Journal of Agricultural and Food Chemistry, Y. Ye, A. Wagh, S. Martini, Using high intensity ultrasound as a tool to change the functional properties of interesterified soybean oil, 59 (2011) 10712–10722., Copyright 2018 American Chemical Society [187].

Based on the previous observations, a mechanism was proposed to explain the action of ultrasound during lipid crystallization which was schematically represented by Martini [189]. After the formation of a supersaturated or undercooled solution, the effect of ultrasound depends on the absence or presence of crystalline material. In the former case, sonication can induce primary nucleation, although the involvement of the cavitation bubbles in this process is not completely understood. In the presence of crystals, ultrasound generates new cavitation-induced nuclei in addition to fragmentation and breakage of the existing crystals. Overall, the ultrasound-assisted crystallization process results in the formation of smaller crystals and a change in physical properties [189].

The work of Wagterveld *et al.* on sonicated precipitation of calcium carbonate also provides a detailed investigation of the effect of ultrasound during different stages of the crystallization process [190,191]. By using five fixed time windows for sonication, the authors were able to discuss the effect of ultrasound on nucleation and early growth. At the start of the experiment ($t=0$), solutions of CaCl_2 and NaHCO_3 were added to the reactor. It is assumed that nucleation starts upon this first formation of supersaturation, although the limited size of the critical nuclei prevents actual detection of the nucleus formation process. Figure 13 shows the progress of the pH and the light scattering index during the precipitation process under five different conditions. Compared to the blank run, performed under silent conditions, application of ultrasound throughout the entire experiment (US 0 – 4500 s) reduces the induction time and increases the volumetric precipitation rate. The latter effect was attributed to a higher number of particles in the reactor under sonicated conditions, resulting in a larger available surface area for growth. Since sonication during the primary nucleation stage (0 – 600 s) did not show any significant effect on the pH and scattering profile compared to the blank experiment, the authors concluded that ultrasound has no significant effect on the amount of primary nuclei. In contrast, the use of sonication during a later stage in which there is a conversion from nuclei to crystals (600 – 1200 s) or during the crystal growth stage (1800 – 2400 s), significantly alters the induction time and volumetric precipitation rate. The authors attributed this effect predominantly to deaggregation of crystals and to a minor extent to particle breakage. Both phenomena are caused by micromixing and shockwave formation which induce shear forces that disrupt the particles, leading to an increase in the available surface area.

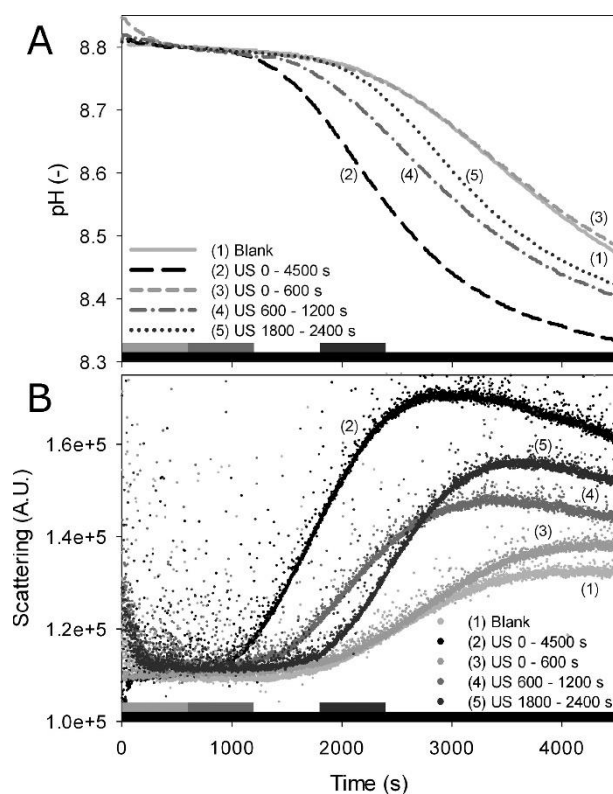


Figure 13: Progress of the precipitation of CaCO_3 monitored by change in pH (A) and light scattering (B) in the absence and presence of ultrasound. Reprinted with permission from Crystal Growth and Design, R.M. Wagterveld, H. Miedema, G. Witkamp, Effect of Ultrasonic Treatment on Early Growth during CaCO_3 Precipitation, (2012) 4403–4410. Copyright 2018 American Chemical Society [190].

In our group, the moment of ultrasound application during crystallization was studied using isothermal cooling crystallization of a 20 g.L^{-1} paracetamol solution in a 30 kHz ultrasonic recirculation setup as the model system [192]. Based on the progress of the supersaturation level, three temporal stages were defined for this process. These stages are represented utilizing the observation of nucleation and complete desupersaturation as boundaries between these stages as schematically represented in Figure 14. This methodology allows to study the effect of ultrasound in both a supersaturated and desupersaturated solution. Similarly to the previous

studies a distinction is made between the effect of ultrasound on supersaturated solutions with and without crystals.

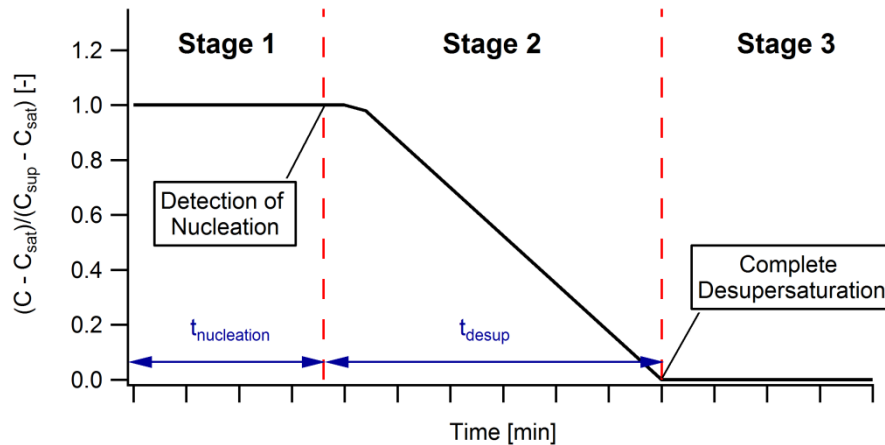


Figure 14: Schematic overview of the progress of the normalized supersaturation level during crystallization and the demarcation of the three stages in which ultrasound is applied. C is the concentration in the solution, C_{sat} is the solubility level and C_{sup} is the initial concentration before nucleation. Reprinted with permission of, Copyright © 2018, John Wiley and Sons [192].

The demarcation between the first and second stage is based on visual detection of nucleation in the solution. Initially detected nuclei are considered as primary crystals, while additional crystal formation after the onset of nucleation is defined as secondary nucleation. Therefore, a comparison of the PSD between samples with application of ultrasound in either stage 1 or 2 is able to demonstrate the effect of sonication on primary and secondary nucleation. In addition, the dominant mechanism for particle size reduction by ultrasound could be identified by comparing the use of ultrasound in one of these stages. In the end, the effect of ultrasound

before and after complete desupersaturation was investigated by comparing sonication stage 2 and 3, respectively. The results of all these experiments are shown in Figure 15 [192].

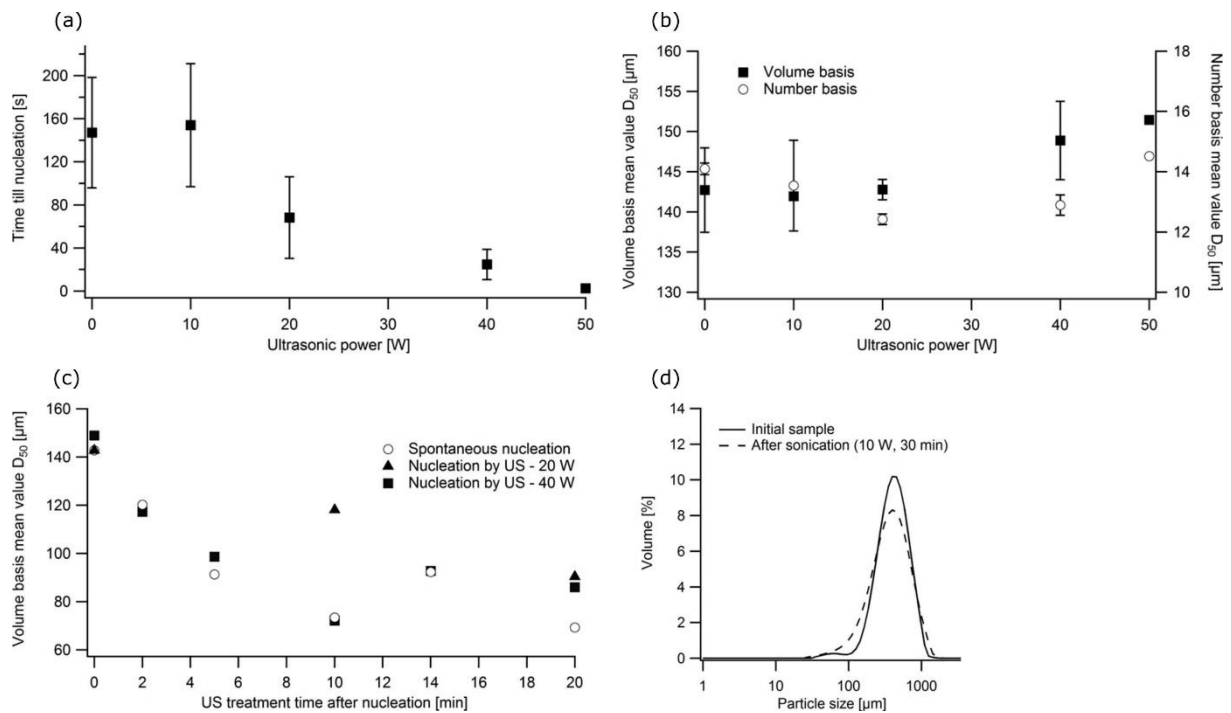


Figure 15: Effect of ultrasound on nucleation and median particle size. Sonication (30 kHz) is applied during different stages of the crystallization process. (a) Effect of ultrasonic power on time till nucleation by sonication during stage 1, (b) Effect on median particle size by sonication during stage 1, (c) Effect on median particle size by sonication during stage 2, (d) Effect on particle size distribution by sonication during stage 3. Reprinted with permission of, Copyright © 2018, John Wiley and Sons [192].

From Figure 15 (a), it is clear that sonication above a threshold of 10 W significantly reduces the induction time and the stochastic nature of the nucleation event, similar as observed by other groups. However, the improved nucleation does not result in the formation of smaller particles as can be derived from the results of Figure 15 (b). Hence, both the volume and number basis

data indicate that application of ultrasound in the first stage yields a similar final particle size, independent of the ultrasonic power and induction time. In contrast, when sonication is enabled in the second stage, after primary nucleation and in the presence of crystals, the particle size can be significantly reduced. By increasing the ultrasonic power and/or exposure time in this second stage, the particle size can be tailored to a desired value, as indicated by Figure 15 (c). Although similar claims were reported by other studies [6,10,95,169,170,181–184], it is important to notice that from this study only the sonication period after nucleation appears to be important for particle size control and not the total treatment time. Hence, application of ultrasound before nucleation will only initiate the process, but does not significantly influence the final particle size. However, in case a very high ultrasonic power is used, nucleation will occur quasi-immediately (Figure 15 (a)), resulting in an inversed-proportional relation between the particle size and the total sonication time, as reported by others. In the end, Figure 15 (d) shows that the crystal size distribution after sonication starts at smaller particle sizes compared to the distribution of the initial sample. This distribution after sonication is obtained by sonicating the initial sample, obtained in stage 3, for 30 min at 10 W. In this stage the solution is completely desupersaturated so that no crystal growth or nucleation can occur anymore. This indicates that sonication of a completely desupersaturated solution will further reduce the median particle size by breakage of the crystals, possibly leading to damaged crystal surfaces along a large amount of fines. In general, the observations from the experiments plotted in Figure 15 are in accordance with the results of Wagterveld *et al.* and Ye *et al.*, claiming that ultrasound does not significantly alters the number of primary nuclei, but predominantly boosts secondary nucleation in the presence of existing crystals which results in a particle size reduction [187–191].

When all the previously discussed results are taken into account, it is possible to summarize the main findings and state some general guidelines on when to apply ultrasound during a crystallization process:

- Sonication of a supersaturated solution containing no crystals will significantly reduce the time till nucleation as well as its stochastic nature compared to the spontaneous process. This effect is most pronounced for processes which operate under low supersaturation levels and are characterized by long and rather irreproducible induction times.
- Application of a short sonication period (< 1 min) after the crystallization process is completed will not significantly alter the crystal size. In case a post-treatment is preferred, a longer sonication time (> 15 min) is required to obtain sufficient breakage and fragmentation of the crystals.
- In case a significant particle size reduction is desired, it is recommended to apply ultrasound after primary nucleation. In the presence of these primary crystals, a combination of cavitation-induced nucleation, breakage and deaggregation will boost secondary nucleation, leading to a large amount of small particles in the reactor. The results from the above mentioned papers suggest that the final particle size is mainly influenced by the secondary nucleation and/or growth rates. Because both the secondary nucleation rate and growth rate are not influenced when ultrasound is switched off after primary nucleation, the final particle size is similar as without sonication. When ultrasound is applied after primary nucleation but before the crystals are grown to their final size (stage 2), it will influence the secondary nucleation rate and possibly the growth rate. As a result, the final particle size is impacted. It should, however, be noted that this assumption needs further investigation. In all above mentioned papers some form of mixing was applied by means of a magnetic stirring bar or overhead impeller. It is possible that ultrasound can still impact the crystal size, especially

during antisolvent crystallization, when applied before the first crystals appear and in the case no other form of mixing is provided.

- Crystallizations which operate under high supersaturation levels, such as precipitation reactions or processes in which the solute solution is directly dispersed into an antisolvent, will often generate nuclei immediately, even under silent conditions. In case sonication is used in these processes, it will be mainly applied in a solution containing primary crystals and, therefore, cause a significant particle size reduction. However, if the sonication period is postponed and crystals are already in their final growth stage, the decrease in size will only be marginal.

It should be noted that the above mentioned guidelines are subject to ultrasound power and frequency.

5. Challenges in sonocrystallization

Despite intensive research in the field of sonocrystallization over the last decades, several aspects are not yet completely understood or require optimization. These challenges prevent the design and development of efficient sonocrystallization processes and reactors and the subsequent scale-up of these systems. The list below provides a non-exhaustive overview of these challenges.

- The mechanism of improved nucleation by ultrasound remains ambiguous, although several hypotheses were proposed. Insight into these fundamentals could allow to optimize the required ultrasonic effects [20,193].

- Only a limited number of publications investigated the effect of ultrasound on secondary nucleation. These few studies indicate that ultrasound could significantly impact secondary nucleation. More work is therefore required to gain more insight in the effects and mechanisms of ultrasound on secondary nucleation.
- Conventional seeded crystallization allows to control the polymorphic form of the crystals by seeding with appropriate seeding material in a particular supersaturation region. Similarly, the kinetically controlled polymorph can be favoured over the thermodynamically stable one by application of ultrasound [77]. Some authors attribute this to interference of ultrasonic waves with the pre-nuclei structuring, enhancing the nucleation rate of a particular configuration and crystal polymorph. However, up till now the results are inconsistent and more understanding is required to use ultrasound as a method for polymorph control [101,104,194,195].
- Several papers evidenced particle size reduction by application of ultrasound during crystallization, but the underlying principle of this effect is not yet clarified. Therefore, it is unclear whether a high number of primary nuclei, or enhanced secondary nucleation and breakage of initially formed crystals is the main cause for the production of smaller crystals. An answer to this question allows to employ ultrasound at the right time in the process, thereby reducing the energy consumption [75,158–161,190,196–198].
- The effect of frequency is intensively studied for sonocrystallization processes and many conflicting suggestions to optimize this parameter arise in literature. However, the configuration of the equipment, the power dissipation and the cavitation bubble type strongly differ among the different experimental setups, making it impossible to generalize the conclusions. Therefore, to determine the effect of frequency, proper characterization of the sound field, the cavitation bubbles and the induced ultrasonic energy is required [77,137,199–201].

- Ultrasound can be operated in continuous or pulsed mode throughout the crystallization process and both modes are exploited throughout many research papers. However, it is not clear how to optimize or operate the latter one since different settings are used by many groups. Pulsed sonication could potentially lower the energy consumption and improve the cavitation effects, as shown in other applications fields such as semiconductor wafer cleaning. Transfer of the knowledge from this research field could possibly benefit sonocrystallization [173,175–180,202].
- One of the most promising assets of ultrasound in crystallization is its ability to avoid seed material as it can directly induce nucleation. Ultrasound could, therefore, provide an alternative way of seeding in sterile processes that usually rely on spontaneous nucleation which is governed by a statistical distribution and thus less predictable. However, in order to apply sonication as a seeding technology, the correlation between the ultrasonic parameters such as power and exposure time, and the particle size has to be studied. Consequently, this will allow to ‘tailor’ the final particle size by adequate setting of the sonication parameters, similar as a change in seed mass can alter these crystal properties [95,184,203].
- Most research on sonocrystallization is performed in lab-scale equipment and provides a proof of principle for the benefits of the technology. Industrial implementation and effective scale-up is, however, lacking although large-scale and high power equipment is already available. In order to promote this technology beyond academic laboratories, research should focus on scale-up strategies and large-scale reactor design [8,200,204–210].

6. Conclusion and perspective

This review shows that ultrasound is a valuable tool to achieve better control over the crystallization process. Ultrasound allows to impact the induction time, particle size distribution and in some cases the crystal shape, polymorphic form and chirality. Most significant and clear effects are observed during nucleation and fragmentation. The effects of ultrasound on crystal growth are often masked by the effects of ultrasound on nucleation and fragmentation. Despite the fact that the effects of ultrasound on the different aspects of the crystallization process are well studied and clear, the mechanisms behind these effects are rarely studied and less understood. Several hypotheses are proposed to explain the effect of ultrasound on nucleation, crystal growth and fragmentation. Further research is, however, needed to clarify which of these hypotheses are plausible. This lack of physically sensible parameters to describe nucleation and growth processes is also one of the main bottlenecks for the development of solid population balance models.

Most papers in literature used commercially available ultrasound equipment with the goal to demonstrate that ultrasound creates improvements of the crystallization process. A small number of researchers designed their own ultrasound setups to investigate and optimize the effect of ultrasound parameters on the crystallization process. As a result, the effect of ultrasound power on the crystallization process is well studied. Most commercially available ultrasound devices allow in particular to control the applied ultrasound power within certain ranges. Generally, the higher the applied power, the stronger the observed effects are. This high power leads, however, to a larger energy demand. Pulsed ultrasound seems to be a promising method to reduce the energy consumption while still obtaining the positive effects of ultrasound. Also the moment of application of ultrasound seems to be an important parameter to consider. Often it is not required to apply ultrasound over the whole period of the crystallization process. In contrast to the ultrasonic power, the frequency is less studied.

Most commercial devices do not allow changes to the applied frequency. Over a small frequency range of tenths of kHz, the differences in the effects observed are rather limited. Over a larger range, from kHz to MHz, however, it seems to be an important parameter. In addition, different trends are sometimes observed between different ultrasound devices and crystallizers. More research is required to define whether these differences are caused by the differences in type of cavitation bubbles or ultrasound source, or both. [The following matrix summarizes the effects of ultrasound parameters on different aspects of crystallization process.](#)

	Frequency	Power (P)	Type of cavitation bubbles	Time window	Moment of application
Nucleation	20-100 kHz ↑ nucleation rate (↓ MZW, ↓ t _{in})	P ↑ => nucleation rate ↑ (↓ MZW, ↓ t _{in} , ↓ stochasticity)	Independent of bubble type	Pulse length ↑ => nucleation rate ↑ (till threshold power)	Before nucleation: ↓ t _{in} ↓ stochastic nature After initial nucleation: →secondary nucleation
Growth	MHz range particle size ↑	P ↑ =>particle size ↑ (when no fragmentation)	?	?	After nucleation before complete desupersaturation
Polymorphism	20 kHz – 18.2 MHz creation of less stable polymorph	?	?	?	During nucleation
Fragmentation /deaggregation	20-100 kHz particle size ↓	P ↑ => fragmentation rate ↑ => particle size ↓	Stable: fracturing Transient: abrasion	Sonication time ↑ => Fragmentation rate ↑ => Particle size ↓	After initial nucleation, during or after desupersaturation
Purity (aromatic components)	affected when: <100 kHz + volatile aromatic components or 165-850 kHz + aromatics with hydrophilic characteristics	P ↑ => degradation ↑ => purity ↓	?	Sonication time ↑ => degradation ↑ => purity ↓	?

Figure 16 Matrix summarizing the effects of ultrasound parameters on different aspects of crystallization process. ? means that no clear effect is reported in literature or no articles were found which investigated this effect

The scale-up of ultrasound assisted crystallization is perhaps one of the greatest challenges for its application in industry [5]. The main reasons for this are the complexity of sonocrystallization which hampers the development of first-principle process models that have predictive capabilities and, secondly, the limited penetration depth of ultrasound. The dissipation of ultrasonic power in a solution is limited to several centimetres [11,12].

Therefore, the ultrasound effects can completely disappear when scaling up to a larger scale. These scale-up issues are particularly problematic when operating crystallization in large batch vessels. However, new opportunities arise when applying ultrasound in continuous crystallization processes as smaller-sized crystallizers can be used while maintaining the same throughput. The current trend in pharmaceutical industry towards continuous manufacturing provides, therefore, new opportunities for application of sonocrystallization on an industrial scale.

Acknowledgements

Christos Xiouras acknowledges funding of a Ph.D. fellowship by the Research Foundation-Flanders (FWO). J. Jordens acknowledges funding of a Ph.D. grant by the Agency for Innovation by Science and Technology (IWT) and the Agency for Innovation and Entrepreneurship (VLAIO) and Catalisti grant number PIF HBC.2017.0442. B. Gielen received funding from the European Community's Seventh Framework Programme (FP7/2007-2013) under grant agreement n° NMP2-SL-2012-309874 (ALTEREGO). This project has received funding from the European Union's Horizon 2020 research and innovation programme under the Marie Skłodowska-Curie grant agreement No 721290. This publication reflects only the author's view, exempting the Community from any liability. Project website: <http://cosmic-etn.eu/>.

References

- [1] R.A. Granberg, D.G. Bloch, Å.C. Rasmuson, Crystallization of paracetamol in acetone–water mixtures, *J. Cryst. Growth*. 198–199 (1999) 1287–1293.
doi:[https://doi.org/10.1016/S0022-0248\(98\)01013-6](https://doi.org/10.1016/S0022-0248(98)01013-6).
- [2] L. Richard, V.N. G., K. Herman, J. Peter, G. Johan, Application of ultrasound for start-up of evaporative batch crystallization of ammonium sulfate in a 75-L crystallizer, *AIChE J.* 57 (n.d.) 3367–3377. doi:10.1002/aic.12553.
- [3] G. Ruecroft, D. Hipkiss, T. Ly, N. Maxted, P.W. Cains, Sonocrystallization: The Use of Ultrasound for Improved Industrial Crystallization, *Org. Process Res. Dev.* 9 (2005) 923–932. doi:10.1021/op050109x.
- [4] A. Myerson, *Handbook of industrial crystallization*, Butterworth-Heinemann, 2002.
- [5] J. Wang, F. Li, R. Lakerveld, Process intensification for pharmaceutical crystallization, *Chem. Eng. Process. - Process Intensif.* 127 (2018) 111–126.
doi:<https://doi.org/10.1016/j.cep.2018.03.018>.
- [6] R.S. Dhumal, S. V Biradar, A.R. Paradkar, P. York, Particle engineering using sonocrystallization: salbutamol sulphate for pulmonary delivery., *Int. J. Pharm.* 368 (2009) 129–37. doi:10.1016/j.ijpharm.2008.10.006.
- [7] R. Ambrus, N.N. Amirzadi, P. Sipos, P. Szabó-Révész, Effect of Sonocrystallization on the Habit and Structure of Gemfibrozil Crystals, *Chem. Eng. Technol.* 33 (2010) 827–832. doi:10.1002/ceat.200900568.
- [8] P.R. Gogate, V.S. Sutkar, A.B. Pandit, Sonochemical reactors: Important design and scale up considerations with a special emphasis on heterogeneous systems, *Chem. Eng.*

- J. 166 (2011) 1066–1082. doi:10.1016/j.cej.2010.11.069.
- [9] V.S. Nalajala, V.S. Moholkar, Investigations in the physical mechanism of sonocrystallization., *Ultrason. Sonochem.* 18 (2011) 345–55.
doi:10.1016/j.ultsonch.2010.06.016.
- [10] A. Abbas, M. Srour, P. Tang, H. Chiou, H.-K. Chan, J.A. Romagnoli, Sonocrystallisation of sodium chloride particles for inhalation, *Chem. Eng. Sci.* 62 (2007) 2445–2453. doi:10.1016/j.ces.2007.01.052.
- [11] T.J. Mason, *Sonochemistry: Timothy J. Mason*, University Press, 1999.
- [12] C. Horst, P.R. Gogate, A.B. Pandit, *Ultrasound Reactors*, in: *Model. Process Intensif.*, Wiley-VCH Verlag GmbH & Co. KGaA, 2007: pp. 193–277.
doi:10.1002/9783527610600.ch8.
- [13] C.E. Brennen, *Cavitation and bubble dynamics*, Cambridge University Press, 2013.
- [14] R.M. Wagterveld, L. Boels, M.J. Mayer, G.J. Witkamp, Visualization of acoustic cavitation effects on suspended calcite crystals., *Ultrason. Sonochem.* 18 (2011) 216–25. doi:10.1016/j.ultsonch.2010.05.006.
- [15] W.T. Richards, A.L. Loomis, THE CHEMICAL EFFECTS OF HIGH FREQUENCY SOUND WAVES I. A PRELIMINARY SURVEY, *J. Am. Chem. Soc.* 49 (1927) 3086–3100. doi:10.1021/ja01411a015.
- [16] C. Bartos, Á. Kukovecz, R. Ambrus, G. Farkas, N. Radacsi, P. Szabó-Révész, Comparison of static and dynamic sonication as process intensification for particle size reduction using a factorial design, *Chem. Eng. Process. Process Intensif.* 87 (2015) 26–34. doi:10.1016/j.cep.2014.10.015.

- [17] J.K. Skrebowski, J. Williamson, Recovery of paraxylene crystals under refrigeration and sonic vibration conditions, (1970).
- [18] Q.T.Z. Ximei, SUGAR CRYSTAL GROWTH FROM SOLUTION UNDER ULTRASOUND TREATMENT CONDITION [J], J. SOUTH CHINA Univ. Technol. (NATURAL Sci. 6 (1996).
- [19] J.R.G. Sander, B.W. Zeiger, K.S. Suslick, Sonocrystallization and sonofragmentation, *Ultrason. Sonochem.* 21 (2014) 1908–1915. doi:10.1016/j.ultsonch.2014.02.005.
- [20] S.L. Hem, The effect of ultrasonic vibrations on crystallization processes, *Ultrasonics.* 5 (1967) 202–207. doi:10.1016/0041-624X(67)90061-3.
- [21] L. de los S. Castillo-Peinado, M.D.L. de Castro, The role of ultrasound in pharmaceutical production: sonocrystallization, *J. Pharm. Pharmacol.* 68 (2016) 1249–1267. doi:10.1111/jphp.12614.
- [22] X. Cheng, M. Zhang, B. Xu, B. Adhikari, J. Sun, The principles of ultrasound and its application in freezing related processes of food materials: A review, *Ultrason. Sonochem.* 27 (2015) 576–585. doi:10.1016/j.ultsonch.2015.04.015.
- [23] M. Dalvi-Isfahan, N. Hamdami, E. Xanthakis, A. Le-Bail, Review on the control of ice nucleation by ultrasound waves, electric and magnetic fields, *J. Food Eng.* 195 (2017) 222–234. doi:10.1016/j.jfoodeng.2016.10.001.
- [24] Z. Zhang, D.-W. Sun, Z. Zhu, L. Cheng, Enhancement of Crystallization Processes by Power Ultrasound: Current State-of-the-Art and Research Advances, *Compr. Rev. Food Sci. Food Saf.* 14 (2015) 303–316. doi:10.1111/1541-4337.12132.
- [25] H.N. Kim, K.S. Suslick, The Effects of Ultrasound on Crystals: Sonocrystallization and

- Sonofragmentation, *Crystals*. 8 (2018). doi:10.3390/cryst8070280.
- [26] S.S. Kadam, Monitoring and Characterization of Crystal Nucleation and Growth during Batch Crystallization, (2012).
- [27] J. Jordens, Application of Acoustic Energy in Crystallization Processes, KU Leuven, 2016.
- [28] B. Gielen, Particle Engineering by Sonocrystallization: Controlling particle size and shape by a targeted application of ultrasound, (2017).
- [29] G. Zeng, H. Li, S. Luo, X. Wang, J. Chen, Effects of ultrasonic radiation on induction period and nucleation kinetics of sodium sulfate, *Korean J. Chem. Eng.* 31 (2014) 807–811.
- [30] Y.H. Kim, K. Lee, K.K. Koo, Y.G. Shul, S. Haam, Comparison Study of Mixing Effect on Batch Cooling Crystallization of 3-Nitro-1,2,4-triazol-5-one (NTO) Using Mechanical Stirrer and Ultrasound Irradiation, *Cryst. Res. Technol.* 37 (2002) 928–944. doi:10.1002/1521-4079(200209)37:9<928::AID-CRAT928>3.0.CO;2-R.
- [31] R. Chow, R. Blindt, R. Chivers, M. Povey, A study on the primary and secondary nucleation of ice by power ultrasound, *Ultrasonics*. 43 (2005) 227–230.
doi:10.1016/j.ultras.2004.06.006.
- [32] Z. Guo, A.G. Jones, H. Hao, B. Patel, N. Li, Effect of ultrasound on the heterogeneous nucleation of BaSO₄ during reactive crystallization, *J. Appl. Phys.* 101 (2007) 54907.
doi:10.1063/1.2472652.
- [33] Z. Guo, A.G. Jones, N. Li, The effect of ultrasound on the homogeneous nucleation of BaSO₄ during reactive crystallization, *Chem. Eng. Sci.* 61 (2006) 1617–1626.

doi:10.1016/j.ces.2005.09.009.

- [34] A.H. Bari, A. Chawla, A.B. Pandit, Sono-crystallization kinetics of K₂SO₄: Estimation of nucleation, growth, breakage and agglomeration kinetics, *Ultrason. Sonochem.* 35 (2017) 196–203. doi:<https://doi.org/10.1016/j.ultsonch.2016.09.018>.
- [35] J.R.G. Sander, B.W. Zeiger, K.S. Suslick, Sonocrystallization and sonofragmentation., *Ultrason. Sonochem.* 21 (2014) 1908–15. doi:10.1016/j.ultsonch.2014.02.005.
- [36] A. Kordylla, T. Krawczyk, F. Tumakaka, G. Schembecker, Modeling ultrasound-induced nucleation during cooling crystallization, *Chem. Eng. Sci.* 64 (2009) 1635–1642. doi:10.1016/j.ces.2008.12.030.
- [37] F. Hu, D.-W. Sun, W. Gao, Z. Zhang, X. Zeng, Z. Han, Effects of pre-existing bubbles on ice nucleation and crystallization during ultrasound-assisted freezing of water and sucrose solution, *Innov. Food Sci. Emerg. Technol.* 20 (2013) 161–166. doi:10.1016/j.ifset.2013.08.002.
- [38] A. Kordylla, S. Koch, F. Tumakaka, G. Schembecker, Towards an optimized crystallization with ultrasound: Effect of solvent properties and ultrasonic process parameters, *J. Cryst. Growth.* 310 (2008) 4177–4184. doi:<http://dx.doi.org/10.1016/j.jcrysgro.2008.06.057>.
- [39] C. Virone, H.J.M. Kramer, G.M. van Rosmalen, A.H. Stoop, T.W. Bakker, Primary nucleation induced by ultrasonic cavitation, *J. Cryst. Growth.* 294 (2006) 9–15. doi:10.1016/j.jcrysgro.2006.05.025.
- [40] A.H. Bari, A. Chawla, A.B. Pandit, Sono-crystallization kinetics of K₂SO₄: Estimation of nucleation, growth, breakage and agglomeration kinetics, *Ultrason. Sonochem.* 35 (2017) 196–203. doi:10.1016/j.ultsonch.2016.09.018.

- [41] J.R.G. Sander, B.W. Zeiger, K.S. Suslick, Sonocrystallization and sonofragmentation, *Ultrason. Sonochem.* 21 (2014) 1908–1915. doi:10.1016/j.ultsonch.2014.02.005.
- [42] A. Kordylla, S. Koch, F. Tumakaka, G. Schembecker, Towards an optimized crystallization with ultrasound: Effect of solvent properties and ultrasonic process parameters, *J. Cryst. Growth.* 310 (2008) 4177–4184. doi:10.1016/j.jcrysgr.2008.06.057.
- [43] T. Hazi Mastan, M. Lenka, D. Sarkar, Nucleation kinetics from metastable zone widths for sonocrystallization of l-phenylalanine, *Ultrason. Sonochem.* 36 (2017) 497–506. doi:10.1016/j.ultsonch.2016.12.017.
- [44] R. Chow, R. Blindt, R. Chivers, M. Povey, The sonocrystallisation of ice in sucrose solutions: primary and secondary nucleation, *Ultrasonics.* 41 (2003) 595–604. doi:10.1016/j.ultras.2003.08.001.
- [45] Z. Guo, M. Zhang, H. Li, J. Wang, E. Kougoulos, Effect of ultrasound on anti-solvent crystallization process, *J. Cryst. Growth.* 273 (2005) 555–563.
- [46] R. Chow, R. Blindt, R. Chivers, M. Povey, A study on the primary and secondary nucleation of ice by power ultrasound., *Ultrasonics.* 43 (2005) 227–30. doi:10.1016/j.ultras.2004.06.006.
- [47] M.D. Luque de Castro, F. Priego-Capote, Ultrasound-assisted crystallization (sonocrystallization), *Ultrason. Sonochem.* 14 (2007) 717–24. doi:10.1016/j.ultsonch.2006.12.004.
- [48] H. Li, J. Wang, Y. Bao, Z. Guo, M. Zhang, Rapid sonocrystallization in the salting-out process, *J. Cryst. Growth.* 247 (2003) 192–198. doi:10.1016/S0022-0248(02)01941-3.

- [49] R. Chow, R. Mettin, B. Lindinger, T. Kurz, W. Lauterborn, The importance of acoustic cavitation in the sonocrystallisation of ice-high speed observations of a single acoustic bubble, *Ultrason. 2003 IEEE Symp.* 2 (2003) 1447–1450 Vol.2.
doi:10.1109/ULTSYM.2003.1293177.
- [50] K. Wohlgemuth, F. Ruether, G. Schembecker, Sonocrystallization and crystallization with gassing of adipic acid, *Chem. Eng. Sci.* 65 (2010) 1016–1027.
doi:10.1016/j.ces.2009.09.055.
- [51] H. Harzali, F. Baillon, O. Louisnard, F. Espitalier, A. Mgaidi, Experimental study of sono-crystallisation of $\text{ZnSO}_4 \cdot 7\text{H}_2\text{O}$, and interpretation by the segregation theory., *Ultrason. Sonochem.* 18 (2011) 1097–106. doi:10.1016/j.ultsonch.2011.03.007.
- [52] M. Wiklund, R. Green, M. Ohlin, Acoustofluidics 14: Applications of acoustic streaming in microfluidic devices, *Lab Chip.* 12 (2012) 2438–2451.
doi:10.1039/C2LC40203C.
- [53] J.C. Colmenares, G. Chatel, *Sonochemistry: from basic principles to innovative applications*, Springer, 2017.
- [54] E.A. Neppiras, Acoustic cavitation, *Phys. Rep.* 61 (1980) 159–251. doi:10.1016/0370-1573(80)90115-5.
- [55] M. Ashokkumar, The characterization of acoustic cavitation bubbles—an overview, *Ultrason. Sonochem.* 18 (2011) 864–872.
- [56] R. Tronson, M. Ashokkumar, F. Grieser, Comparison of the Effects of Water-Soluble Solutes on Multibubble Sonoluminescence Generated in Aqueous Solutions by 20- and 515-kHz Pulsed Ultrasound, *J. Phys. Chem. B.* 106 (2002) 11064–11068.
doi:10.1021/jp020363g.

- [57] B.W. Zeiger, K.S. Suslick, Sonofragmentation of molecular crystals, *J. Am. Chem. Soc.* 133 (2011) 14530–14533.
- [58] H. Kiani, D.-W. Sun, A. Delgado, Z. Zhang, Investigation of the effect of power ultrasound on the nucleation of water during freezing of agar gel samples in tubing vials., *Ultrason. Sonochem.* 19 (2012) 576–81. doi:10.1016/j.ultsonch.2011.10.009.
- [59] A. Brothie, F. Grieser, M. Ashokkumar, Effect of Power and Frequency on Bubble-Size Distributions in Acoustic Cavitation, *Phys. Rev. Lett.* 102 (2009) 84302. <http://link.aps.org/doi/10.1103/PhysRevLett.102.084302>.
- [60] J. Jordens, B. Gielen, L. Braeken, T. Van Gerven, Determination of the effect of the ultrasonic frequency on the cooling crystallization of paracetamol, *Chem. Eng. Process. Process Intensif.* 84 (2014) 38–44. doi:10.1016/j.cep.2014.01.006.
- [61] H. Kiani, Z. Zhang, A. Delgado, D.-W. Sun, Ultrasound assisted nucleation of some liquid and solid model foods during freezing, *Food Res. Int.* 44 (2011) 2915–2921. doi:10.1016/j.foodres.2011.06.051.
- [62] X. Zhang, T. Inada, A. Tezuka, Ultrasonic-induced nucleation of ice in water containing air bubbles, *Ultrason. Sonochem.* 10 (2003) 71–76. doi:10.1016/S1350-4177(02)00151-7.
- [63] C. Cogné, S. Labouret, R. Peczalski, O. Louisnard, F. Baillon, F. Espitalier, Theoretical model of ice nucleation induced by acoustic cavitation. Part 1: Pressure and temperature profiles around a single bubble, *Ultrason. Sonochem.* 29 (2016) 447–454. doi:<https://doi.org/10.1016/j.ultsonch.2015.05.038>.
- [64] C. Cogné, S. Labouret, R. Peczalski, O. Louisnard, F. Baillon, F. Espitalier, Theoretical model of ice nucleation induced by inertial acoustic cavitation. Part 2: Number of ice

- nuclei generated by a single bubble, *Ultrason. Sonochem.* 28 (2016) 185–191.
doi:<https://doi.org/10.1016/j.ultsonch.2015.07.019>.
- [65] K. Wohlgemuth, A. Kordylla, F. Ruether, G. Schembecker, Experimental study of the effect of bubbles on nucleation during batch cooling crystallization, *Chem. Eng. Sci.* 64 (2009) 4155–4163. doi:10.1016/j.ces.2009.06.041.
- [66] J. Dodds, F. Espitalier, O. Louisnard, R. Grossier, R. David, M. Hassoun, F. Baillon, C. Gatamel, N. Lyczko, The Effect of Ultrasound on Crystallisation-Precipitation Processes: Some Examples and a New Segregation Model, *Part. Part. Syst. Charact.* 24 (2007) 18–28. doi:10.1002/ppsc.200601046.
- [67] O. Louisnard, F.J. Gomez, R. Grossier, Segregation of a liquid mixture by a radially oscillating bubble, *J. Fluid Mech.* 577 (2007) 385. doi:10.1017/S002211200700479X.
- [68] H.-L. Cao, D.-C. Yin, Y.-Z. Guo, X.-L. Ma, J. He, W.-H. Guo, X.-Z. Xie, B.-R. Zhou, Rapid crystallization from acoustically levitated droplets, *J. Acoust. Soc. Am.* 131 (2012) 3164–3172. doi:10.1121/1.3688494.
- [69] S. Patel, Z. Murthy, Anti-solvent sonocrystallisation of lactose, *Chem. Process Eng.* 32 (2011) 379–389. doi:<https://doi.org/10.2478/v10176-011-0030-6>.
- [70] S.R. Patel, Z.V.P. Murthy, Effect of process parameters on crystal size and morphology of lactose in ultrasound-assisted crystallization, *Cryst. Res. Technol.* 46 (2011) 243–248. doi:10.1002/crat.201000694.
- [71] D.J. Kirwan, C.J. Orella, *Handbook of Industrial Crystallization*, Elsevier, 2002.
<http://www.sciencedirect.com/science/article/pii/B9780750670128500136>.
- [72] A. Cacciuto, S. Auer, D. Frenkel, Onset of heterogeneous crystal nucleation in

- colloidal suspensions, *Nature*. 428 (2004) 404–406.
<http://dx.doi.org/10.1038/nature02397>.
- [73] X.-H. Guo, S.-H. Yu, Controlled Mineralization of Barium Carbonate Mesocrystals in a Mixed Solvent and at the Air/Solution Interface Using a Double Hydrophilic Block Copolymer as a Crystal Modifier, *Cryst. Growth Des.* 7 (2007) 354–359.
doi:10.1021/cg060575t.
- [74] I. Kuzmenko, H. Rapaport, K. Kjaer, J. Als-Nielsen, I. Weissbuch, M. Lahav, L. Leiserowitz, Design and Characterization of Crystalline Thin Film Architectures at the Air–Liquid Interface: Simplicity to Complexity, *Chem. Rev.* 101 (2001) 1659–1696.
doi:10.1021/cr990038y.
- [75] R. Chow, R. Blindt, R. Chivers, M. Povey, The sonocrystallisation of ice in sucrose solutions: primary and secondary nucleation, *Ultrasonics*. 41 (2003) 595–604.
doi:10.1016/j.ultras.2003.08.001.
- [76] K.A. Ramisetty, A.B. Pandit, P.R. Gogate, Ultrasound-Assisted Antisolvent Crystallization of Benzoic Acid: Effect of Process Variables Supported by Theoretical Simulations, *Ind. Eng. Chem. Res.* 52 (2013) 17573–17582. doi:10.1021/ie402203k.
- [77] S. Kaur Bhangu, M. Ashokkumar, J. Lee, Ultrasound Assisted Crystallization of Paracetamol: Crystal Size Distribution and Polymorph Control, *Cryst. Growth Des.* 16 (2016) 1934–1941. doi:10.1021/acs.cgd.5b01470.
- [78] A. Moghtada, A. Shahrouzianfar, R. Ashiri, Low-temperature ultrasound synthesis of nanocrystals CoTiO₃ without a calcination step: Effect of ultrasonic waves on formation of the crystal growth mechanism, *Adv. Powder Technol.* 28 (2017) 1109–1117. doi:<https://doi.org/10.1016/j.appt.2016.11.004>.

- [79] W.N. Al Nasser, K. Pitt, M.J. Hounslow, Monitoring of aggregation and scaling of calcium carbonate in the presence of ultrasound irradiation using focused beam reflectance measurement, *Powder Technol.* 238 (2013) 151–160.
doi:10.1016/j.powtec.2012.03.021.
- [80] S. Nii, S. Takayanagi, Growth and size control in anti-solvent crystallization of glycine with high frequency ultrasound., *Ultrason. Sonochem.* 21 (2014) 1182–6.
doi:10.1016/j.ultsonch.2013.11.009.
- [81] V.I. Rodchenkov, D.A. Sergeev, Fluid flows induced by focused ultrasound and their use in single-crystal growth, *J. Appl. Mech. Tech. Phys.* 50 (2009) 553–557.
doi:10.1007/s10808-009-0074-2.
- [82] J. Jordens, B. Bamps, B. Gielen, L. Braeken, T. Van Gerven, The effects of ultrasound on micromixing, *Ultrason. Sonochem.* 32 (2016) 68–78.
doi:10.1016/j.ultsonch.2016.02.020.
- [83] J. Jordens, T. Appermont, B. Gielen, T. Van Gerven, L. Braeken, Sonofragmentation: Effect of Ultrasound Frequency and Power on Particle Breakage, *Cryst. Growth Des.* 16 (2016) 6167–6177. doi:10.1021/acs.cgd.6b00088.
- [84] T.D. Dincer, B. Zisu, C.G.M.R. Vallet, V. Jayasena, M. Palmer, M. Weeks, Sonocrystallisation of lactose in an aqueous system, *Int. Dairy J.* 35 (2014) 43–48.
doi:https://doi.org/10.1016/j.idairyj.2013.10.001.
- [85] J. Lee, M. Ashokkumar, S.E. Kentish, Influence of mixing and ultrasound frequency on antisolvent crystallisation of sodium chloride, *Ultrason. Sonochem.* 21 (2014) 60–68.
doi:http://dx.doi.org/10.1016/j.ultsonch.2013.07.005.
- [86] R.S. Vishwakarma, P.R. Gogate, Intensified oxalic acid crystallization using ultrasonic

- reactors: Understanding effect of operating parameters and type of ultrasonic reactor, *Ultrason. Sonochem.* 39 (2017) 111–119.
doi:<https://doi.org/10.1016/j.ultsonch.2017.04.015>.
- [87] O. Hussein, A. Ali, S. Mourtada, R.J. A., Effects of operating conditions on particle size in sonocrystallization, *Asia-Pacific J. Chem. Eng.* 5 (n.d.) 599–608.
doi:10.1002/apj.437.
- [88] E. Kougoulos, I. Marziano, P.R. Miller, Lactose particle engineering: Influence of ultrasound and anti-solvent on crystal habit and particle size, *J. Cryst. Growth.* 312 (2010) 3509–3520. doi:10.1016/j.jcrysgr.2010.09.022.
- [89] B. Pohl, R. Jamshidi, G. Brenner, U.A. Peuker, Experimental study of continuous ultrasonic reactors for mixing and precipitation of nanoparticles, *Chem. Eng. Sci.* 69 (2012) 365–372. doi:10.1016/j.ces.2011.10.058.
- [90] R. OVSHINSKY, Stanford, R. YOUNG, ULTRASONIC METHOD FOR FORMING SPHERICAL NICKEL HYDROXIDE, 1997.
- [91] N. Belkacem, M.A. Sheikh Salem, H.S. AlKhatib, Effect of ultrasound on the physico-chemical properties of poorly soluble drugs: Antisolvent sonocrystallization of ketoprofen, *Powder Technol.* 285 (2015) 16–24.
doi:<https://doi.org/10.1016/j.powtec.2015.06.058>.
- [92] T. BYRNE, M.P. DAHAL, TRANSITION METAL COMPOUND PARTICLES AND METHODS OF PRODUCTION, 2012.
- [93] J. Jordens, N. De Coker, B. Gielen, T. Van Gerven, L. Braeken, Ultrasound precipitation of manganese carbonate: The effect of power and frequency on particle properties, *Ultrason. Sonochem.* 26 (2015) 64–72. doi:10.1016/j.ultsonch.2015.01.017.

- [94] B. Gielen, Y. Thimmesch, J. Jordens, G. Janssen, L.C.J. Thomassen, T. Van Gerven, L. Braeken, Ultrasonic precipitation of manganese carbonate: Reactor design and scale-up, *Chem. Eng. Res. Des.* 115 (2016). doi:10.1016/j.cherd.2016.09.012.
- [95] H. Li, H. Li, Z. Guo, Y. Liu, The application of power ultrasound to reaction crystallization, *Ultrason. Sonochem.* 13 (2006) 359–363.
doi:10.1016/j.ultsonch.2006.01.002.
- [96] T. Prozorov, R. Prozorov, K.S. Suslick, High Velocity Interparticle Collisions Driven by Ultrasound, *J. Am. Chem. Soc.* 126 (2004) 13890–13891. doi:10.1021/ja049493o.
- [97] K.S. Suslick, S.J. Doktycz, E.B. Flint, On the origin of sonoluminescence and sonochemistry, *Ultrasonics.* 28 (1990) 280–290. doi:https://doi.org/10.1016/0041-624X(90)90033-K.
- [98] L.-X. Yang, Y.-J. Zhu, H. Tong, W.-W. Wang, Submicrocubes and highly oriented assemblies of MnCO₃ synthesized by ultrasound agitation method and their thermal transformation to nanoporous Mn₂O₃, *Ultrason. Sonochem.* 14 (2007) 259–265.
doi:https://doi.org/10.1016/j.ultsonch.2006.05.006.
- [99] P.-H. Kuo, B.-C. Zhang, C.-S. Su, J.-J. Liu, M.-T. Sheu, Application of two-level factorial design to investigate the effect of process parameters on the sonocrystallization of sulfathiazole, *J. Cryst. Growth.* 471 (2017) 8–14.
doi:https://doi.org/10.1016/j.jcrysgr.2017.04.035.
- [100] H. Hatakka, H. Alatalo, M. Louhi-Kultanen, I. Lassila, E. Hæggröm, Closed-Loop Control of Reactive Crystallization PART II: Polymorphism Control of L-Glutamic Acid by Sonocrystallization and Seeding, *Chem. Eng. Technol.* 33 (2010) 751–756.
doi:10.1002/ceat.200900577.

- [101] M. Louhi-Kultanen, M. Karjalainen, J. Rantanen, M. Huhtanen, J. Kallas, Crystallization of glycine with ultrasound, *Int. J. Pharm.* 320 (2006) 23–29. doi:10.1016/j.ijpharm.2006.03.054.
- [102] I. Yuki, H. Izumi, Polymorph Control of L-ArgHCl on Antisolvent Crystallization by Ultrasonic Irradiation, *Chem. Eng. Technol.* 40 (2017) 1318–1322. doi:10.1002/ceat.201600678.
- [103] I. Yuki, H. Izumi, Polymorph Control of L-Phenylalanine in Cooling Crystallization by Ultrasonication, *Chem. Eng. Technol.* 0 (2018). doi:10.1002/ceat.201700662.
- [104] S. Gracin, M. Uusi-Penttilä, Å.C. Rasmuson, Influence of ultrasound on the nucleation of polymorphs of p-aminobenzoic acid, *Cryst. Growth Des.* 5 (2005) 1787–1794. doi:10.1021/cg050056a.
- [105] R.M. Santos, P. Ceulemans, T. Van Gerven, Synthesis of pure aragonite by sonochemical mineral carbonation, *Chem. Eng. Res. Des.* 90 (2012) 715–725. doi:https://doi.org/10.1016/j.cherd.2011.11.022.
- [106] K. Renuka Devi, A. Raja, K. Srinivasan, Ultrasound assisted nucleation and growth characteristics of glycine polymorphs – A combined experimental and analytical approach, *Ultrason. Sonochem.* 24 (2015) 107–113. doi:https://doi.org/10.1016/j.ultsonch.2014.11.006.
- [107] J. Jordens, E. Canini, B. Gielen, T. Van Gerven, L. Braeken, Ultrasound assisted particle size control by continuous seed generation and batch growth, *Crystals.* 7 (2017). doi:10.3390/cryst7070195.
- [108] C. Bai, C. Wang, T. Zheng, Q. Hu, Growth of [small beta]-glycine crystals promoted by standing surface acoustic waves (SSAWs), *CrystEngComm.* 20 (2018) 1245–1251.

doi:10.1039/C7CE02038D.

[109] Y. Song, W. Chen, X. Chen, Ultrasonic Field Induced Chiral Symmetry Breaking of NaClO₃ Crystallization, *Cryst. Growth Des.* 8 (2008) 1448–1450.

doi:10.1021/cg701072r.

[110] D.D. Medina, A. Gedanken, Y. Mastai, Chiral amplification in crystallization under ultrasound radiation, *Chem. - A Eur. J.* 17 (2011) 11139–11142.

doi:10.1002/chem.201101221.

[111] X. Zhou, H. Wang, Q. Zeng, Chiral separation of <sc>dl</sc>-glutamic acid by ultrasonic field, *CrystEngComm.* 19 (2017) 762–766. doi:10.1039/C6CE02027E.

[112] C. Viedma, Chiral symmetry breaking during crystallization: Complete chiral purity induced by nonlinear autocatalysis and recycling, *Phys. Rev. Lett.* 94 (2005) 3–6.

doi:10.1103/PhysRevLett.94.065504.

[113] W.L. Noorduin, T. Izumi, A. Millemaggi, M. Leeman, H. Meekes, W.J.P. Van Enkevort, R.M. Kellogg, B. Kaptein, E. Vlieg, D.G. Blackmond, Emergence of a Single Solid Chiral State from a Nearly Racemic Amino Acid Derivative, *J. Am. Chem. Soc.* 130 (2008) 1158–1159. doi:10.1021/ja7106349.

[114] C. Rougeot, F. Guillen, J.-C. Plaquevent, G. Coquerel, Ultrasound-Enhanced Deracemization: Toward the Existence of Agonist Effects in the Interpretation of Spontaneous Symmetry Breaking, *Cryst. Growth Des.* (2015) 150324151109006.

doi:10.1021/cg501765g.

[115] C. Xiouras, A. Fytopoulos, J. Jordens, A.G. Boudouvis, T. Van Gerven, G.D. Stefanidis, Applications of ultrasound to chiral crystallization, resolution and deracemization, *Ultrason. Sonochem.* 43 (2018). doi:10.1016/j.ultsonch.2018.01.014.

- [116] J.X. Gao, H.Q. Huang, X.X. Li, F.H. Du, L.B. Li, J.S. Li, Breakage and Particle Size Redistribution in an Ultrasound-Intensified Leaching Process, *Chem. Eng. Technol.* 38 (2015) 1665–1670. doi:10.1002/ceat.201400703.
- [117] V. Raman, A. Abbas, Experimental investigations on ultrasound mediated particle breakage., *Ultrason. Sonochem.* 15 (2008) 55–64. doi:10.1016/j.ultsonch.2006.11.009.
- [118] H.N. Kim, K.S. Suslick, Sonofragmentation of Ionic Crystals, *Chem. – A Eur. J.* 23 (2017) 2778–2782. doi:10.1002/chem.201605857.
- [119] A.H. Bari, A.B. Pandit, Ultrasound-facilitated particle breakage: Estimation of kinetic parameters using population balance modelling, *Can. J. Chem. Eng.* 92 (2014) 2046–2052.
- [120] C. Xiouras, A.A. Fytopoulos, J.H. Ter Horst, A.G. Boudouvis, T. Van Gerven, G.D. Stefanidis, Particle Breakage Kinetics and Mechanisms in Attrition-Enhanced Deracemization, *Cryst. Growth Des.* 18 (2018) 3051–3061. doi:10.1021/acs.cgd.8b00201.
- [121] A.N. Ivanov, Ultrasonic dispersion of Al–AlN and Al₂O₃ nanopowder agglomerates and of nanostructured AlOOH particles, *Russ. Phys. J.* 54 (2012) 1413–1417. doi:10.1007/s11182-012-9763-z.
- [122] O. Kudryashova, S. Vorozhtsov, On the Mechanism of Ultrasound-Driven Deagglomeration of Nanoparticle Agglomerates in Aluminum Melt, *JOM.* 68 (2016) 1307–1311. doi:10.1007/s11837-016-1851-z.
- [123] B. Gielen, J. Jordens, L.C.J. Thomassen, L. Braeken, T. Van Gerven, Agglomeration control during ultrasonic crystallization of an active pharmaceutical ingredient, *Crystals.* 7 (2017). doi:10.3390/cryst7020040.

- [124] L.G. Austin, A review Introduction to the mathematical description of grinding as a rate process.pdf, *Powder Technol.* 5 (1971) 1–17. doi:10.1016/0032-5910(71)80064-5.
- [125] L.E. Patruno, C.A. Dorao, H.F. Svendsen, H.A. Jakobsen, Analysis of breakage kernels for population balance modelling, *Chem. Eng. Sci.* 64 (2009) 501–508. doi:10.1016/j.ces.2008.09.029.
- [126] K.A. Kusters, S.E. Pratsinis, S.G. Thoma, D.M. Smith, Ultrasonic fragmentation of agglomerate powders, *Chem. Eng. Sci.* 48 (1993) 4119–4127. doi:10.1016/0009-2509(93)80258-R.
- [127] M.L. Rasche, *Mathematical Modeling, Simulation and Optimal Design of Pharmaceutical Crystallizers*, (2015).
- [128] J.P. Guillemain, E. Schaer, P. Marchal, C. Lemaître, H. Nonnet, A. Ledieu, A mass conservative approach to model the ultrasonic de-agglomeration of ZnO nanoparticle suspension in water, *Powder Technol.* 219 (2012) 59–64. doi:10.1016/j.powtec.2011.12.009.
- [129] C. Engineering, C. Engineering, Comparison Study of Mixing Effect on Batch Cooling Crystallization of 3-Nitro-1, 2, 4-triazol-5-one (NTO) Using, (2002) 928–944.
- [130] Narducci O., PhD Thesis - Particle engineering via sonocrystallization: the aqueous adipic acid system., Univerity Coll. London - Dep. Chem. Eng. (2012).
- [131] S. Jiang, An Examination of Sonocrystallization Kinetics of L-Glutamic Acid, (2012) 182.
- [132] C.D. Mateescu, R. Isopescu, F. Branzoi, M. Mihai, I. Chilibon, Precipitation of super-fine calcium carbonate by controlled double jet method: Solid phase characterization

- and estimation of kinetic parameters, *J. Optoelectron. Adv. Mater.* 10 (2008) 2667–2674.
- [133] A. Kordylla, T. Krawczyk, F. Tumakaka, G. Schembecker, Modeling ultrasound-induced nucleation during cooling crystallization, *Chem. Eng. Sci.* 64 (2009) 1635–1642. doi:10.1016/j.ces.2008.12.030.
- [134] K. Wohlgemuth, G. Schembecker, Modeling induced nucleation processes during batch cooling crystallization: A sequential parameter determination procedure, *Comput. Chem. Eng.* 52 (2013) 216–229. doi:10.1016/j.compchemeng.2012.12.001.
- [135] S. Bhoi, D. Sarkar, Modelling and experimental validation of ultrasound assisted unseeded batch cooling crystallization of <sc>l</sc>-asparagine monohydrate, *CrystEngComm.* 18 (2016) 4863–4874. doi:10.1039/C6CE00937A.
- [136] T. Yamaguchi, M. Nomura, T. Matsuoka, S. Koda, Effects of frequency and power of ultrasound on the size reduction of liposome., *Chem. Phys. Lipids.* 160 (2009) 58–62. doi:10.1016/j.chemphyslip.2009.04.002.
- [137] J. Jordens, B. Gielen, L. Braeken, T. Van Gerven, Determination of the effect of the ultrasonic frequency on the cooling crystallization of paracetamol, *Chem. Eng. Process. Process Intensif.* 84 (2014). doi:10.1016/j.cep.2014.01.006.
- [138] G.N. Kozhemyakin, L. V Zolkina, Y. Inatomi, Influence of Ultrasound on Crystal Growth from Solution and Related Flow Visualization, *Cryst. Growth Des.* 6 (2006) 2412–2416. doi:10.1021/cg0499313.
- [139] J. Jordens, B. Bamps, B. Gielen, L. Braeken, T. Van Gerven, The effects of ultrasound on micromixing, *Ultrason. Sonochem.* 32 (2016). doi:10.1016/j.ultsonch.2016.02.020.

- [140] F. Parvizian, M. Rahimi, M. Faryadi, Macro- and micromixing in a novel sonochemical reactor using high frequency ultrasound, *Chem. Eng. Process. Process Intensif.* 50 (2011) 732–740. doi:10.1016/j.cep.2011.06.011.
- [141] M. Jagannathan, F. Grieser, M. Ashokkumar, Sonophotocatalytic degradation of paracetamol using TiO₂ and Fe³⁺, *Sep. Purif. Technol.* 103 (2013) 114–118. doi:<https://doi.org/10.1016/j.seppur.2012.10.003>.
- [142] I. Quesada-Peñate, C. Julcour Lebigue, U.J. Jáuregui Haza, A.-M. Wilhelm, H. Delmas, Sonolysis of levodopa and paracetamol in aqueous solutions, *Ultrason. Sonochem.* 16 (2009) 610–616. doi:10.1016/j.ultsonch.2008.11.008.
- [143] Y.G. Adewuyi, *Sonochemistry: Environmental Science and Engineering Applications*, *Ind. Eng. Chem. Res.* 40 (2001) 4681–4715. doi:10.1021/ie010096l.
- [144] T.J. Mason, A.P. Newman, S.S. Phull, *Sonochemistry in water treatment*, in: 2nd Int. Conf. Adv. Water Effl. Treat., Professional Engineering Publishing, 1993: pp. 243–250.
- [145] T.I. Mason, J. Lorimer, *Sonochemistry, Theory, Applications and Uses of Ultrasound in Chemistry*, (1988).
- [146] D. Sunartio, M. Ashokkumar, F. Grieser, Study of the Coalescence of Acoustic Bubbles as a Function of Frequency, Power, and Water-Soluble Additives, *J. Am. Chem. Soc.* 129 (2007) 6031–6036. doi:10.1021/ja068980w.
- [147] H. Zhao, J.-X. Wang, Q.-A. Wang, J.-F. Chen, J. Yun, Controlled Liquid Antisolvent Precipitation of Hydrophobic Pharmaceutical Nanoparticles in a Microchannel Reactor, *Ind. Eng. Chem. Res.* 46 (2007) 8229–8235. doi:10.1021/ie070498e.

- [148] J.M. Jiju, Application of advanced oxidation processes for the degradation of organic water pollutants, Mahtama Gandhi University, 2000.
- [149] T. Leighton, *The Acoustic Bubble*, Academic Press, London, 1994.
- [150] C.K. Holland, R.E. Apfel, Thresholds for transient cavitation produced by pulsed ultrasound environment, 88 (1990) 2059–2069.
- [151] T.. Leighton, Bubble population phenomena in acoustic cavitation, *Ultrason. Sonochem.* 2 (1995) S123–S136.
- [152] A. Harkin, A. Nadim, T.J. Kaper, On acoustic cavitation of slightly subcritical bubbles, *Phys. Fluids.* 11 (1980) 274–287.
- [153] B. Gielen, J. Jordens, Y. Thimmesch, L. Thomassen, T. Van Gerven, L. Braeken, Ultrasound precipitation of manganese carbonate: a comparison between low frequency ultrasonic sources, (2014).
- [154] B. Gielen, J. Jordens, J. Janssen, H. Pfeiffer, M. Wevers, L.C.J. Thomassen, L. Braeken, T. Van Gerven, Characterization of stable and transient cavitation bubbles in a milliflow reactor using a multibubble sonoluminescence quenching technique, *Ultrason. Sonochem.* 25 (2015) 31–39. doi:10.1016/j.ultsonch.2014.08.013.
- [155] M. Ashokkumar, J. Lee, Y. Iida, K. Yasui, T. Kozuka, T. Tuziuti, A. Towata, The detection and control of stable and transient acoustic cavitation bubbles, *Phys. Chem. Chem. Phys.* 11 (2009) 10118. doi:10.1039/b915715h.
- [156] J. Lee, K. Yasui, T. Tuziuti, T. Kozuka, A. Towata, Y. Iida, Spatial Distribution Enhancement of Sonoluminescence Activity by Altering Sonication and Solution Conditions, *J. Phys. Chem. B.* 112 (2008) 15333–15341. doi:10.1021/jp8060224.

- [157] M.-W. Park, S.-D. Yeo, Antisolvent Crystallization of Roxithromycin and the Effect of Ultrasound, *Sep. Sci. Technol.* 45 (2010) 1402–1410.
doi:10.1080/01496391003689538.
- [158] R. Chow, R. Blindt, R. Chivers, M. Povey, A study on the primary and secondary nucleation of ice by power ultrasound, *Ultrasonics*. 43 (2005) 227–230.
doi:10.1016/j.ultras.2004.06.006.
- [159] M. Kurotani, E. Miyasaka, S. Ebihara, I. Hirasawa, Effect of ultrasonic irradiation on the behavior of primary nucleation of amino acids in supersaturated solutions, *J. Cryst. Growth*. 311 (2009) 2714–2721. doi:<https://doi.org/10.1016/j.jcrysgr.2009.03.009>.
- [160] E. Miyasaka, Y. Kato, M. Hagsawa, I. Hirasawa, Effect of ultrasonic irradiation on the number of acetylsalicylic acid crystals produced under the supersaturated condition and the ability of controlling the final crystal size via primary nucleation, *J. Cryst. Growth*. 289 (2006) 324–330. doi:<https://doi.org/10.1016/j.jcrysgr.2005.11.084>.
- [161] E. Miyasaka, S. Ebihara, I. Hirasawa, Investigation of primary nucleation phenomena of acetylsalicylic acid crystals induced by ultrasonic irradiation—ultrasonic energy needed to activate primary nucleation, *J. Cryst. Growth*. 295 (2006) 97–101.
doi:<https://doi.org/10.1016/j.jcrysgr.2006.07.020>.
- [162] B. Gielen, P. Kusters, J. Jordens, L.C.J. Thomassen, T. Van Gerven, L. Braeken, Energy efficient crystallization of paracetamol using pulsed ultrasound, *Chem. Eng. Process. Process Intensif.* 114 (2017). doi:10.1016/j.cep.2017.01.001.
- [163] T. Horie, S. Akao, T. Suzuki, K. Tanaka, N. Jia, K. Taniya, S. Nishiyama, N. Ohmura, Process Development for Ultrasonic Fracturing of Zirconium Phosphate Particles, *J. Chem. Eng. JAPAN*. 47 (2014) 124–129. doi:10.1252/jcej.13we087.

- [164] S. Gracin, Å.C. Rasmuson, Polymorphism and crystallization of p-aminobenzoic acid, *Cryst. Growth Des.* 4 (2004) 1013–1023.
- [165] P. Parimaladevi, S. Supriya, K. Srinivasan, The role of ultrasound in controlling the liquid-liquid phase separation and nucleation of vanillin polymorphs I and II, *J. Cryst. Growth.* 484 (2018) 21–30.
- [166] T.J. Mason, A. Tiehm, *Advances in Sonochemistry, Volume 6: Ultrasound in Environmental Protection*, Elsevier, 2001.
- [167] G. Mark, A. Tauber, R. Laupert, H.-P. Schuchmann, D. Schulz, A. Mues, C. von Sonntag, OH-radical formation by ultrasound in aqueous solution – Part II: Terephthalate and Fricke dosimetry and the influence of various conditions on the sonolytic yield, *Ultrason. Sonochem.* 5 (1998) 41–52. doi:10.1016/S1350-4177(98)00012-1.
- [168] S. Kim, C. Wei, S. Kiang, Crystallization process development of an active pharmaceutical ingredient and particle engineering via the use of ultrasonics and temperature cycling, *Org. Process Res. Dev.* 7 (2003) 997–1001.
- [169] O. Narducci, A.G. Jones, E. Kougoulos, An Assessment of the Use of Ultrasound in the Particle Engineering of Micrometer-Scale Adipic Acid Crystals, *Cryst. Growth Des.* 11 (2011) 1742–1749. doi:10.1021/cg1016593.
- [170] O. Narducci, A.G. Jones, Seeding in Situ the Cooling Crystallization of Adipic Acid using Ultrasound, *Cryst. Growth Des.* 12 (2012) 1727–1735.
- [171] J. Li, Y. Bao, J. Wang, Effects of sonocrystallization on the crystal size distribution of cloxacillin benzathine crystals, *Chem. Eng. Technol.* 36 (2013) 1341–1346. doi:10.1002/ceat.201200726.

- [172] M.D. Luque de Castro, F. Priego-Capote, Ultrasound-assisted crystallization (sonocrystallization), *Ultrason. Sonochem.* 14 (2007) 717–724.
doi:10.1016/j.ultsonch.2006.12.004.
- [173] L.J. McCausland, Production of crystalline materials by using high intensity ultrasound, US 7,244,307 B2, 2007.
- [174] P.R. Gogate, S. Shaha, L. Csoka, Intensification of cavitation activity in the sonochemical reactors using gaseous additives, *Chem. Eng. J.* 239 (2014) 364–372.
doi:10.1016/j.cej.2013.11.004.
- [175] L.J. McCausland, P.W. Cains, Power Ultrasound - a Means to Promote and Control Crystallization in Biotechnology, *Biotechnol. Genet. Eng. Rev.* 21 (2004).
- [176] L.J. Mccausland, P.W. Cains, P.D. Martin, Use the Power of Sonocrystallization for Improved Properties, *Fluids Solids Handl.* (2001) 56–61.
- [177] A. Henglein, M. Gutierrez, Chemical effects of continuous and pulsed ultrasound: a comparative study of polymer degradation and iodide oxidation, *J. Phys. Chem.* 94 (1990) 5169–5172. doi:10.1021/j100375a073.
- [178] P.-K. Choi, Y. Kaneko, T. Meguro, Enhancement of Sonoluminescence and Bubble Dynamics using Pulsed Ultrasound at 103 kHz, *Jpn. J. Appl. Phys.* 47 (2008) 4111–4114. doi:10.1143/JJAP.47.4111.
- [179] V. Ciaravino, H.G. Flynn, M.W. Miller, Pulsed enhancement of acoustic cavitation: A postulated model, *Ultrasound Med. Biol.* 7 (1981) 159–166. doi:10.1016/0301-5629(81)90005-3.
- [180] O. Louisnard, F. Espitalier, Sono-crystallization: from experimental results to

- microscopical interpretations, 19th Int. Congr. Acoust. Congr. Acoust. (2007) 2–7.
- [181] U.N. Hatkar, P.R. Gogate, Ultrasound assisted cooling crystallization of sodium acetate, *Ind. Eng. Chem. Res.* 51 (2012) 12901–12909. doi:10.1021/ie202220q.
- [182] O. Narducci, A.G. Jones, E. Kougoulos, Continuous crystallization of adipic acid with ultrasound, *Chem. Eng. Sci.* 66 (2011) 1069–1076. doi:10.1016/j.ces.2010.12.008.
- [183] A.R. Sheikh, S.R. Patel, Ultrasound assisted reactive crystallization of strontium sulfate, *J. Cryst. Growth.* 390 (2014) 114–119. doi:10.1016/j.jcrysgro.2013.11.029.
- [184] C.-S. Su, C.-Y. Liao, W.-D. Jheng, Particle Size Control and Crystal Habit Modification of Phenacetin Using Ultrasonic Crystallization, *Chem. Eng. Technol.* 38 (2015) 181–186. doi:10.1002/ceat.201300573.
- [185] H.-J. Kim, S.-D. Yeo, Liquid antisolvent crystallization of griseofulvin from organic solutions, *Chem. Eng. Res. Des.* 97 (2015) 68–76.
doi:<https://doi.org/10.1016/j.cherd.2015.03.016>.
- [186] U.N. Hatkar, P.R. Gogate, Process intensification of anti-solvent crystallization of salicylic acid using ultrasonic irradiations, *Chem. Eng. Process. Process Intensif.* 57–58 (2012) 16–24. doi:10.1016/j.cep.2012.04.005.
- [187] Y. Ye, A. Wagh, S. Martini, Using high intensity ultrasound as a tool to change the functional properties of interesterified soybean oil, *J. Agric. Food Chem.* 59 (2011) 10712–10722. doi:10.1021/jf202495b.
- [188] Y. Ye, Effect of High Intensity Ultrasound on Crystallization Behavior and Functional Properties of Lipids, Utah State University, 2015.
- [189] S. Martini, Ultrasound in Food Processing: Effect of ultrasound on the physicochemical

- properties of lipids, in: M. Villamiel, A. Montilla, J.V. García-Pérez, J.A. Gárcel, J. Benedito (Eds.), *Ultrasound Food Process. Recent Adv.*, John Wiley & Sons, Ltd, Chichester, UK, 2017: pp. 464–484. doi:10.1002/9781118964156.ch18.
- [190] R.M. Wagterveld, H. Miedema, G. Witkamp, Effect of Ultrasonic Treatment on Early Growth during CaCO₃ Precipitation, *Cryst. Growth Des.* 12 (2012) 4403–4410. doi:10.1021/cg3005882.
- [191] M.R. Wagterveld, *Effect of ultrasound on calcium carbonate crystallization*, Delft University of Technology, 2013.
- [192] B. Gielen, T. Claes, J. Janssens, J. Jordens, L.C.J. Thomassen, T. Van Gerven, L. Braeken, Particle size control during ultrasonic cooling crystallization of paracetamol, *Chem. Eng. Technol.* (2017). doi:10.1002/ceat.201600647.
- [193] K. Wohlgemuth, *Induced Nucleation Processes during Batch Cooling Crystallization*, TU Dortmund, 2012.
- [194] K. Higaki, S. Ueno, T. Koyano, K. Sato, Effects of ultrasonic irradiation on crystallization behavior of tripalmitoylglycerol and cocoa butter, *J. Am. Oil Chem. Soc.* 78 (2001) 513–518. doi:10.1007/s11746-001-0295-y.
- [195] A.A. Thorat, S. V Dalvi, Particle formation pathways and polymorphism of curcumin induced by ultrasound and additives during liquid antisolvent precipitation, *CrystEngComm.* 16 (2014) 11102–11114.
- [196] C.N. Nanev, A. Penkova, Nucleation and growth of lysozyme crystals under external electric field, *Colloids Surfaces A Physicochem. Eng. Asp.* 209 (2002) 139–145. doi:10.1016/S0927-7757(02)00175-9.

- [197] H.W. Anderson, J.B. Carberry, H.F. Staunton, B.C. Sutradhar, Crystallization of adipic acid, US 5,471,001, 1995.
- [198] S. Bechtel, M. Rauls, R. Van Gelder, S.C. Simpson, Crystallization of amino acids using ultrasonic agitation, US 6,992,216 B2, 2006.
- [199] P.R. Gogate, P. a. Tatake, P.M. Kanthale, A.B. Pandit, Mapping of sonochemical reactors: Review, analysis, and experimental verification, *AIChE J.* 48 (2002) 1542–1560. doi:10.1002/aic.690480717.
- [200] A. Kumar, P.R. Gogate, A.B. Pandit, Mapping the efficacy of new designs for large scale sonochemical reactors., *Ultrason. Sonochem.* 14 (2007) 538–44. doi:10.1016/j.ultsonch.2006.11.005.
- [201] T.J. Mason, J.P. Lorimer, D.M. Bates, Y. Zhao, Dosimetry in sonochemistry: the use of aqueous terephthalate ion as a fluorescence monitor, *Ultrason. Sonochem.* 1 (1994) S91–S95. doi:10.1016/1350-4177(94)90004-3.
- [202] M. Hauptmann, Removal of nanoparticles from surfaces using ultrasound at megahertz frequencies: Understanding and controlling acoustic cavitation in a megasonic cleaning system, KULeuven, 2012.
- [203] O. Narducci, Particle Engineering via Sonocrystallization: the aqueous adipic acid system, University College London, 2013.
- [204] T.J. Mason, Industrial sonochemistry: potential and practicality, *Ultrasonics.* 30 (1992) 192–196. doi:10.1016/0041-624X(92)90072-T.
- [205] P.R. Gogate, S. Mujumdar, A.B. Pandit, Large-scale sonochemical reactors for process intensification: Design and experimental validation, *J. Chem. Technol. Biotechnol.* 78

- (2003) 685–693. doi:10.1002/jctb.697.
- [206] T.Y. Wu, N. Guo, C.Y. Teh, J.X.W. Hay, Challenges and Recent Developments of Sonochemical Processes, in: *Adv. Ultrasound Technol. Environ. Remediat.*, 2013: pp. 109–120. doi:10.1007/978-94-007-5533-8.
- [207] Y. Son, M. Lim, J. Khim, Investigation of acoustic cavitation energy in a large-scale sonoreactor, *Ultrason. Sonochem.* 16 (2009) 552–556. doi:10.1016/j.ultsonch.2008.12.004.
- [208] V.S. Sutkar, P.R. Gogate, Design aspects of sonochemical reactors: Techniques for understanding cavitation activity distribution and effect of operating parameters, *Chem. Eng. J.* 155 (2009) 26–36. doi:10.1016/j.cej.2009.07.021.
- [209] O. Dahlem, J. Reisse, V. Halluin, The radially vibrating horn: a scaling up possibility for sonochemical reactions, *Chem. Eng. Sci.* 54 (1999) 2829–2838. doi:10.1016/S0009-2509(98)00356-X.
- [210] U.S. Bhirud, P.R. Gogate, A.M. Wilhelm, A.B. Pandit, Ultrasonic bath with longitudinal vibrations: A novel configuration for efficient wastewater treatment, *Ultrason. Sonochem.* 11 (2004) 143–147. doi:10.1016/j.ultsonch.2004.01.010.